BSC Strut Arrangement Analysis

Ruslan Kurdyumov, Tej Bhadbhade
Ginzton Lab
Stanford University
LIGO-T1100347-v2

July 5, 2011

Abstract

Using FEA modal analysis, we have determined the optimal strut arrangements for BSC2, BSC4, BSC7, and BSC8. In choosing optimal strut arrangements, we have chosen to minimize modal mass and maximize modal frequency for the lowest two structural modes.

The optimal strut arrangement for BSC7 and BSC8, the most space constrained of the chambers, has two short extended struts, one medium extended strut, and one medium inward strut (configuration BSC7B). This configuration has a much higher second modal frequency and modal masses that are at least 10% lower than the next best arrangement.

The optimal strut arrangement for BSC2 has 4 extended struts, two short and two medium (configuration BSC2B). This arrangement has first and second modes that are 5 Hz and 12 Hz higher, respectively, than the 'rowboat' arrangement (configuration BSC2H). However, a case can be made for the 'rowboat' arrangement since its modal masses are $\sim 10\%$ lower.

The best strut arrangement found could only fit into BSC4 - 4 extended medium struts. This arrangement has first and second modes that are 15 Hz and 20 Hz higher, respectively, than the 'rowboat' arrangement. It also has slightly lower modal mass than the original 'rowboat' arrangement.

Although each modal analysis found up to 70 modes below 1000 Hz, most of these modes had negligible modal mass. We did, however, find two significant modes near 300 Hz and 500 Hz. The 300 Hz mode mainly involved motion near the middle of structure, with significant deformation along the single cross-bracing element. The 500 Hz mode was due to loose fixed supports on the structural base (in simulation) causing the structure to move in the vertical direction. This simulated mode was greatly reduced with more firm fixed support conditions.

We did not find any strut modes with significant modal mass.

Contents

1 Introduction

We have conducted a full investigation of the possible beam splitter strut arrangements to use in the BSC chambers. There are four unique table layouts in the chambers, as seen in Figure 1. BSC4 has the most strut arrangement design flexibility, in terms of space constraints. BSC2 is almost as flexible, but BSC7 and BSC8 have much tighter space constraints because of the ITMs. We consider three possible struts, labeled short, medium, and large, which correspond to 12° (D1003277), 30° (D1100445), and 45° (D090001) inclinations from the vertical.

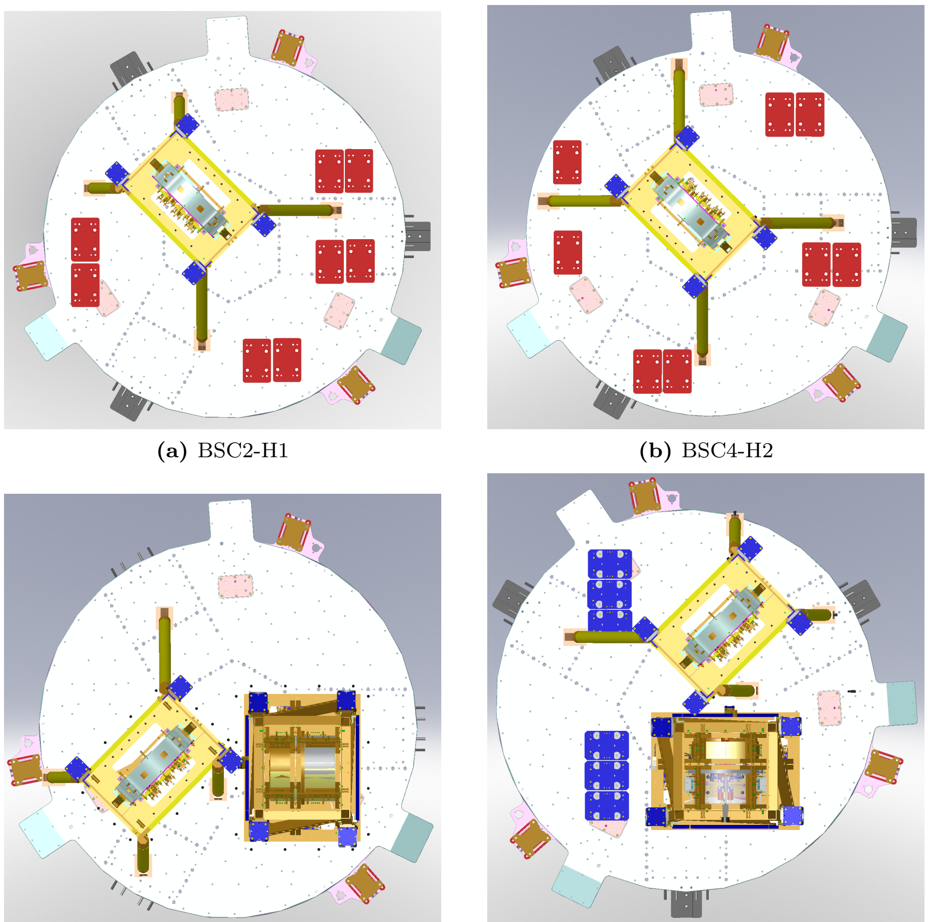

(a) BSC2-H1

(b) BSC4-H2

(c) BSC7-H2

(d) BSC8-H2

Figure 1: [Bottom view] Unique BSC table arrangements that include the beam splitter/folding mirror cage structure. Note that the beam splitter (light yellow) is mirrored from BSC7 to BSC8. BSC2 and BSC4 have much fewer space constraints for strut arrangement design. Some of the bulk trim masses were temporarily removed to make room for struts, and will need to be relocated.

1.1 Simulation Assumptions

We performed FEA modal analysis using ANSYS Workbench, which allowed us to directly import Solidworks models of the beam splitter cage. We used the following settings (all unlisted sections used default settings):

- Geometry

1. Stainless steel for stay leg table interface and fasteners, aluminum for everything else.
2. An 8kg point mass centered on the top plane of the structure, used to model all attachments.

- Connections

1. Bonded contacts between the side plates and small rectangular patches around each bolt hole to more accurately simulate the connection between the side plate and the structure.

- Modal

1. Max Modes to Find: 200.
2. Limit Search to Range: 20 Hz to 1000 Hz.
3. Fixed support at the bottom face of the stay leg table interfaces to simulate the dog clamping of the struts.
4. Fixed support at 4 short edges on the bottom of the structure, as shown in Figure 2, to simulate the dog clamping of the structural base.

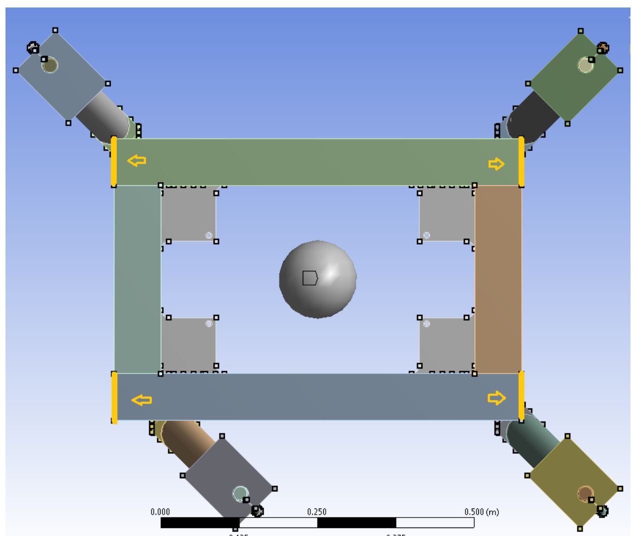

Figure 2: [Bottom view] Fixed edges of structure used for ANSYS FEA analysis (shown in yellow)

2 Preliminary Work

2.1 Side Plate Comparisons

Before analyzing the struts, we had to finalize the beam splitter cage mechanical design. This involved FEA analysis of several new side plate designs, created to make mechanical assembly of the beam splitter easier. The original design, as well as the new designs, are shown in Figure 3. We found that the circular hole design was the best in terms of preserving modal behavior. However, the slotted design was chosen since it offered more room for assembly. Therefore all further analysis will assume the slotted plate is used. The full side plate discussion is included in the Appendix.

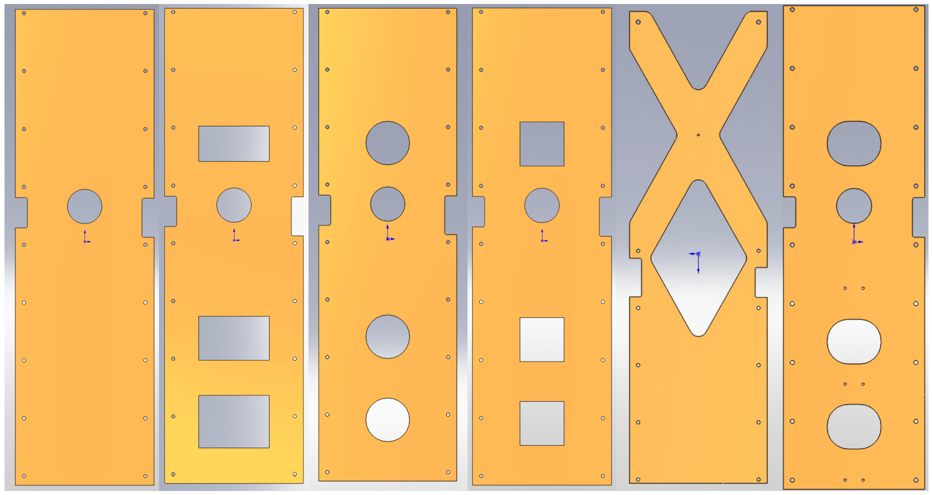

(a) Nominal **(b)** Rectangles **(c)** Circles **(d)** Squares **(e)** Criss-cross **(f)** Slots

Figure 3: Possible side plate designs for the beam splitter cage. The slotted design (D080503-v3) was ulimately chosen over the nominal (D080503-v2) because of improved assembly accessibility and minimal effects on modal behavior.

3 BSC7/BSC8 Possible Strut Arrangements

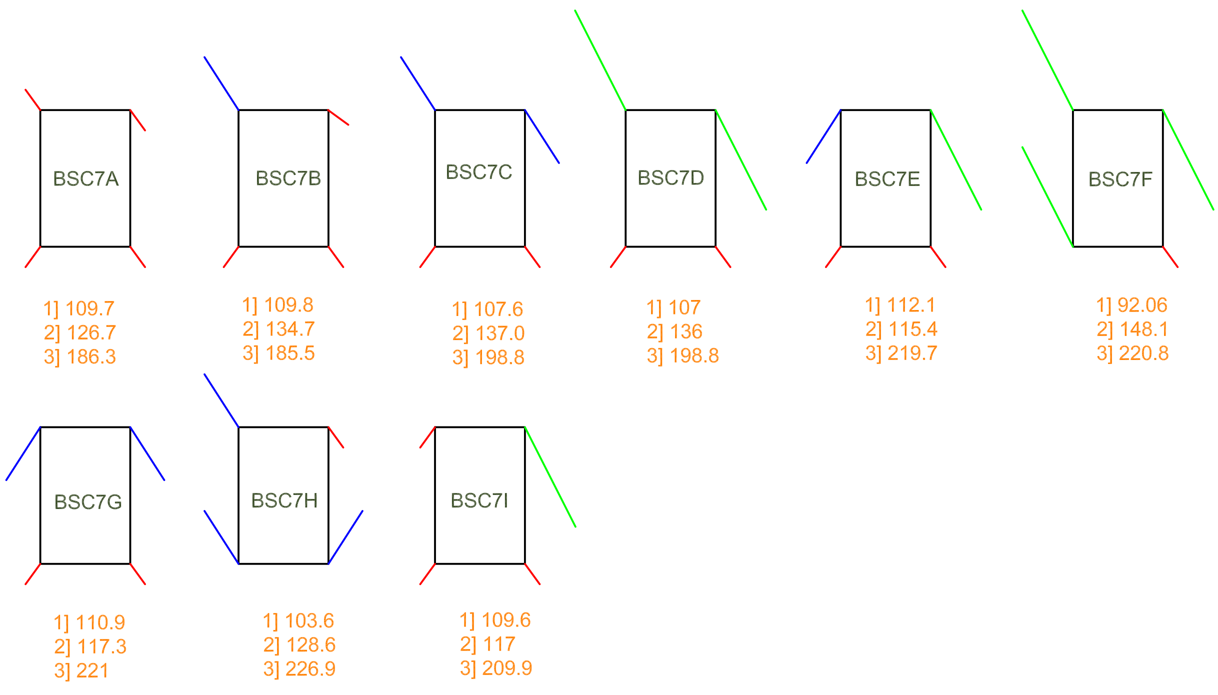

Figure 4: Possible strut arrangements considered for BSC7/BSC8 using the short, medium, and large struts. Each arrangement is labeled and has the lowest three modal frequencies listed.

Since BSC7 and BSC8 had the most stringent space constraints, we fully examined the possible strut arrangements for these chambers first. All the strut arrangements that fit into these chambers can also be used in BSC2 and BSC4. The strut arrangements considered are shown in Figure 4. Since the FM/BS location on the table is mirrored in these chambers, the strut space constraints are identical.

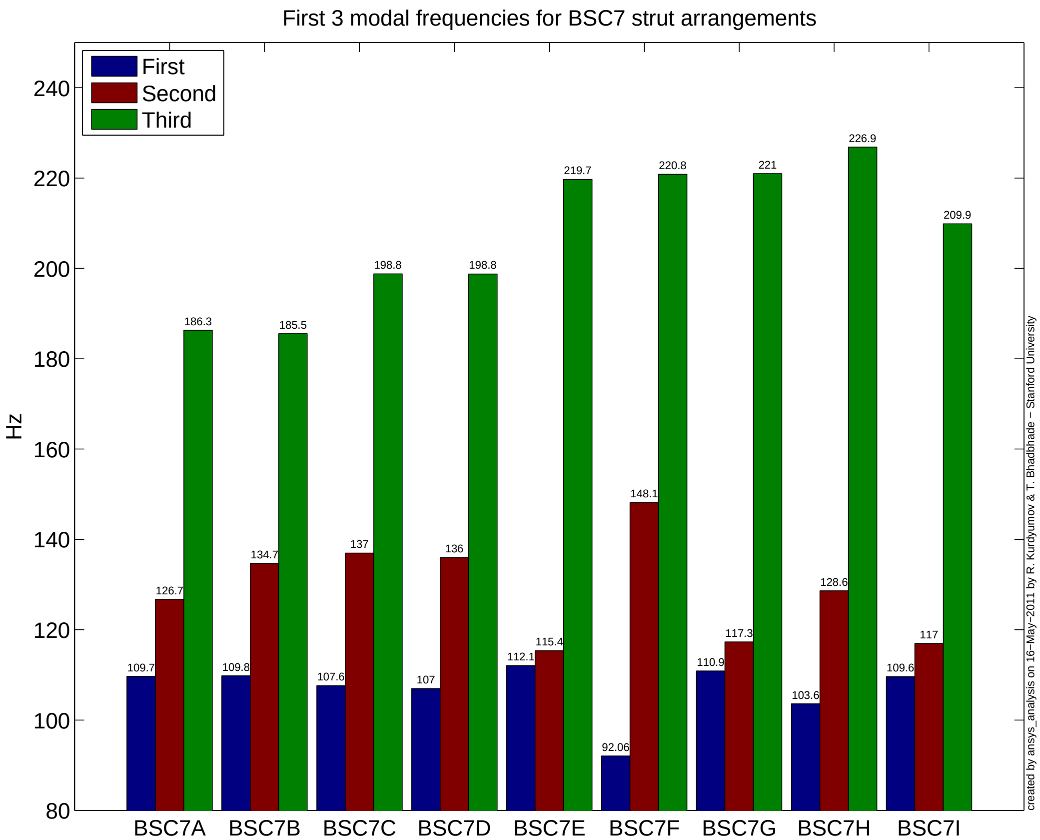

Figure 5: Lowest three modal frequencies for BSC7/BSC8 strut arrangements. A, B, E and G have the best modal behavior.

Using the ANSYS modal analysis, we found the lowest three modal frequencies for each strut arrangement, shown in Figure 5. These modes correspond to longitudinal, lateral and torsional motion of the structure. BSC7A, BSC7B, BSC7E and BSC7G have the best modal behavior for the lower two modes. A and B have a higher 2nd mode, while E has the highest 1st mode.

To test the contribution of each mode to overall structural deformation, we examined the effective masses returned for each mode by ANSYS. Note that ANSYS reports effective mass in the x, y, z directions (and rotational in rotx, roty, rotz), so we used quadrature scaling, $\sqrt{x^2 + y^2 + z^2}$, to get an "overall" effective mass for translation and rotation. For simplicity, we only display the most promising strut arrangements: A, B, E and G. In the next two subsections, we only present the effective modal masses. For the full results, including modal masses for each DOF, as well as cumulative mass fractions, see the Appendix.

3.1 Translational Modal Mass Results

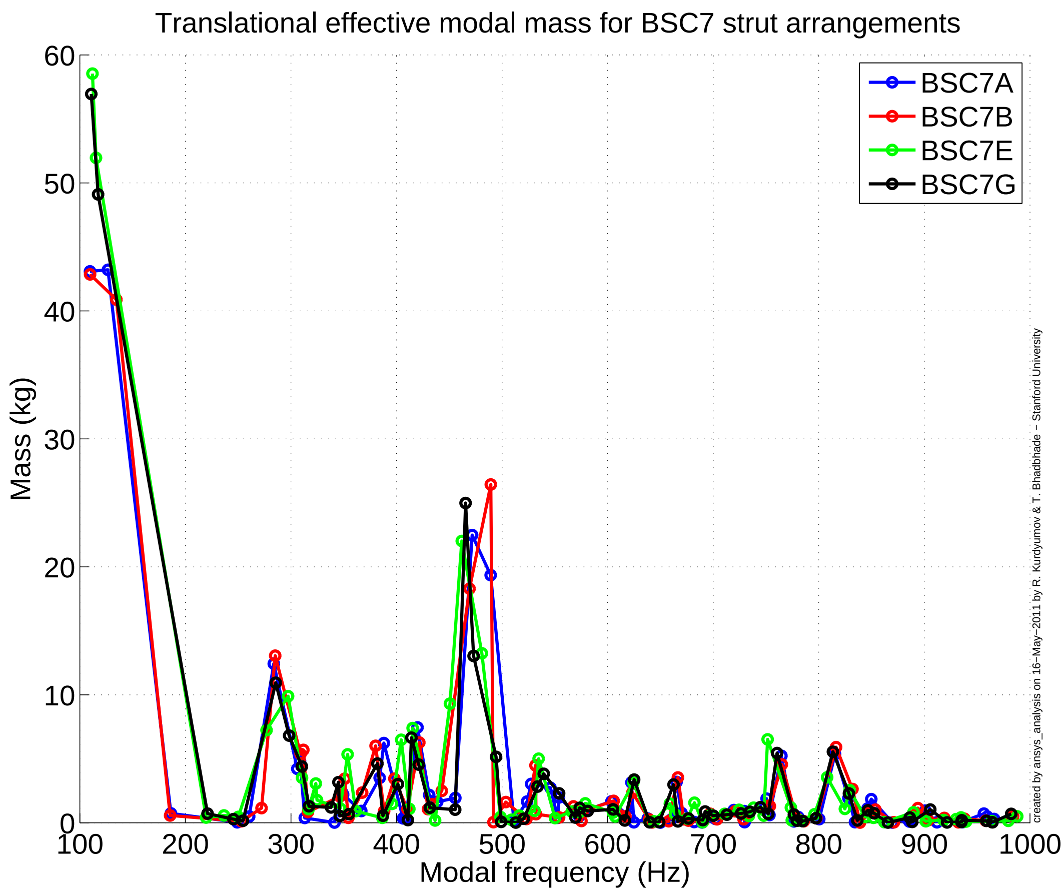

Figure 6: Translational effective mass for each mode (selected BSC7 strut arrangements). The lowest two modes have the highest modal mass, as expected. The large spike just below 500 Hz is an artifact of the fixed support conditions chosen in simulation, which will be discussed later.

The translational effective masses are shown in Figure 6. The first two modes, longitudinal and lateral, have the highest modal mass. This modal mass is substantial, since it's about half of the structure's overall mass (around 118 kg). Therefore, they will contribute most to the structure's overall motion. Note that the modal mass for each 3 extended strut configuration (A and B) is significantly lower than the modal mass for the 'rowboat' style configurations (E and G).

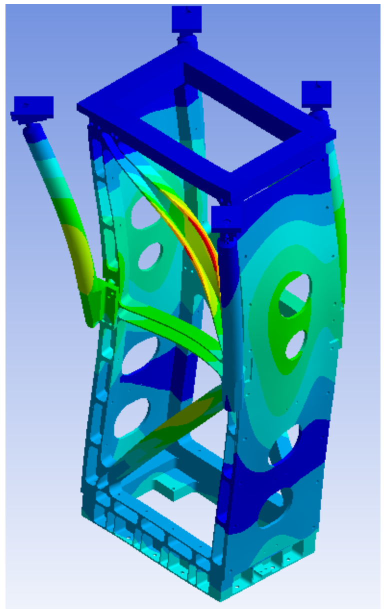

Figure 7: Total deformation caused by mode just below 300 Hz (BSC7A shown)

The next signficant mode is just below 300 Hz. The deformation caused by this mode can be seen in Figure 7. The largest deformation is near the middle of the structure, mostly carried by the single cross-bracing element turned yellow-red. Therefore, this mode appears to be inherent to the structural design and not simply an artifact of simulation setting choices.

There is another significant mode just below 500 Hz. This mode is actually caused by our choice of fixed supports. See the Varying Fixed Supports section for a discussion on this mode.

Finally, we have two minor, but still significant, modes around 760 Hz and 820 Hz. These modes are also caused by our choice of fixed supports and will be discussed in the Varying Fixed Supports section.

3.2 Rotational Modal Mass Results

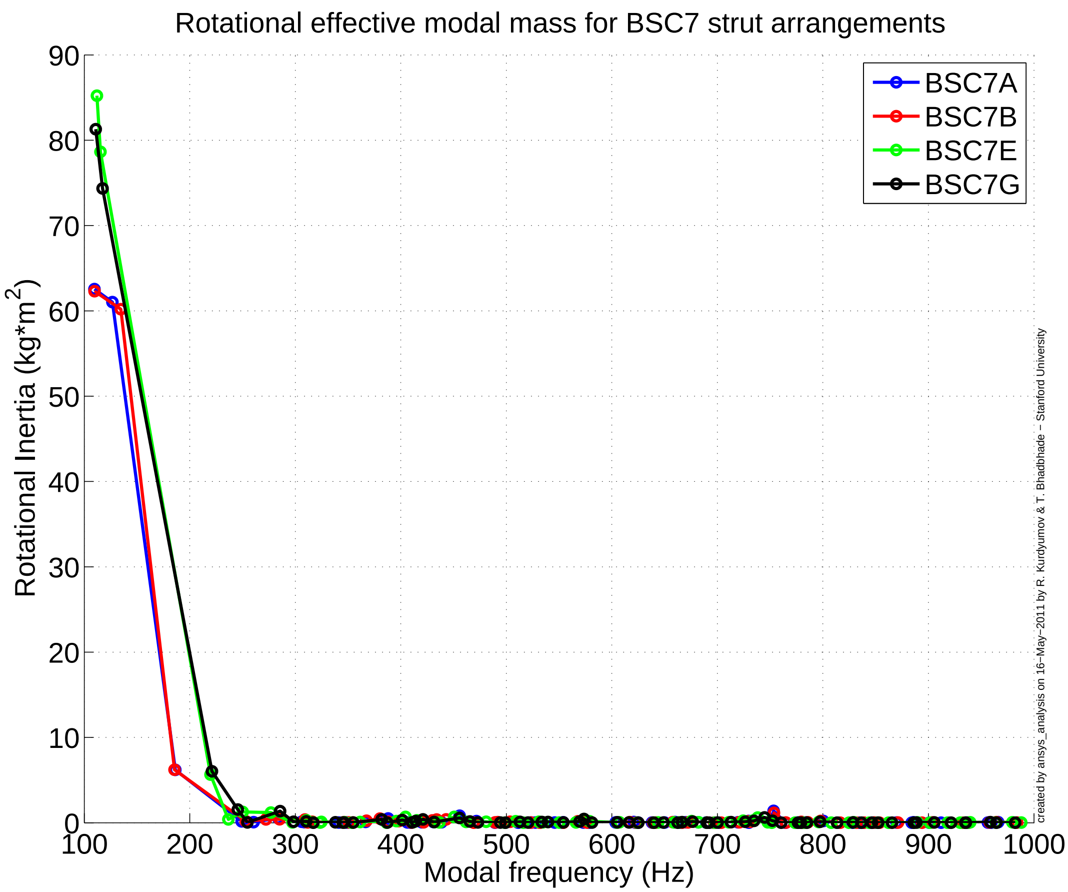

Figure 8: Rotational effective mass for each mode (selected BSC2 strut arrangements). The lowest three modes have the highest modal mass, as expected.

The rotational effective masses are shown in Figure 8. The first three modes capture all of the significant rotation of the structure. Although we would expect the 3rd mode (torsional) to dominate the rotational effective mass, since torsional rotation is about the structure's vertical axis, the rotational moment of inertia for this mode is much less than it is for the longitudinal and lateral modes (which are rotating about a line going through the center of mass of the structure, near the centroid). An important observation is that raising the first two modes of the structure should be prioritized.

Again, BSC7A and BSC7B have significantly lower modal mass.

3.3 Summary

Based on the analysis, we recommend the BSC7A or BSC7B strut arrangements. These arrangements have the largest number of extended struts (3). Although BSC7E and BSC7G have slightly higher frequencies for the first mode, their second mode is significantly worse. Moreover, the modal mass analysis shows that BSC7A and BSC7B have $>10\%$ improvements in modal mass (translational and rotational) for the lower two frequencies.

4 BSC2 Possible Strut Arrangements

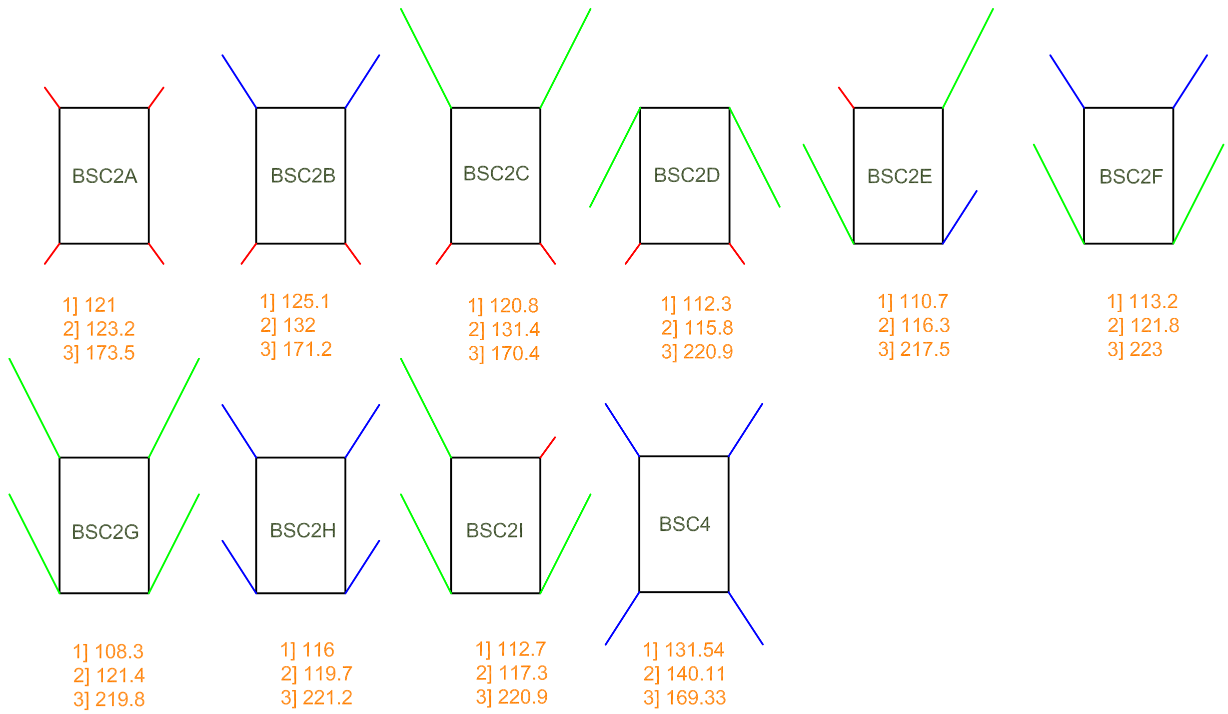

Figure 9: Possible strut arrangements considered for BSC2 using the short, medium, and large struts. Each arrangement is labeled and has the lowest three modal frequencies listed. An additional strut arrangement possible only in BSC4 is also included for reference.

Next, we examined BSC2 strut arrangements. All the BSC7 strut arrangements are valid here, but given looser space constraints, we expect to find improved designs. The additional possible strut arrangements considered are shown in Figure 9. We have also included a strut arrangement only possible in BSC4: 4 medium extended struts.

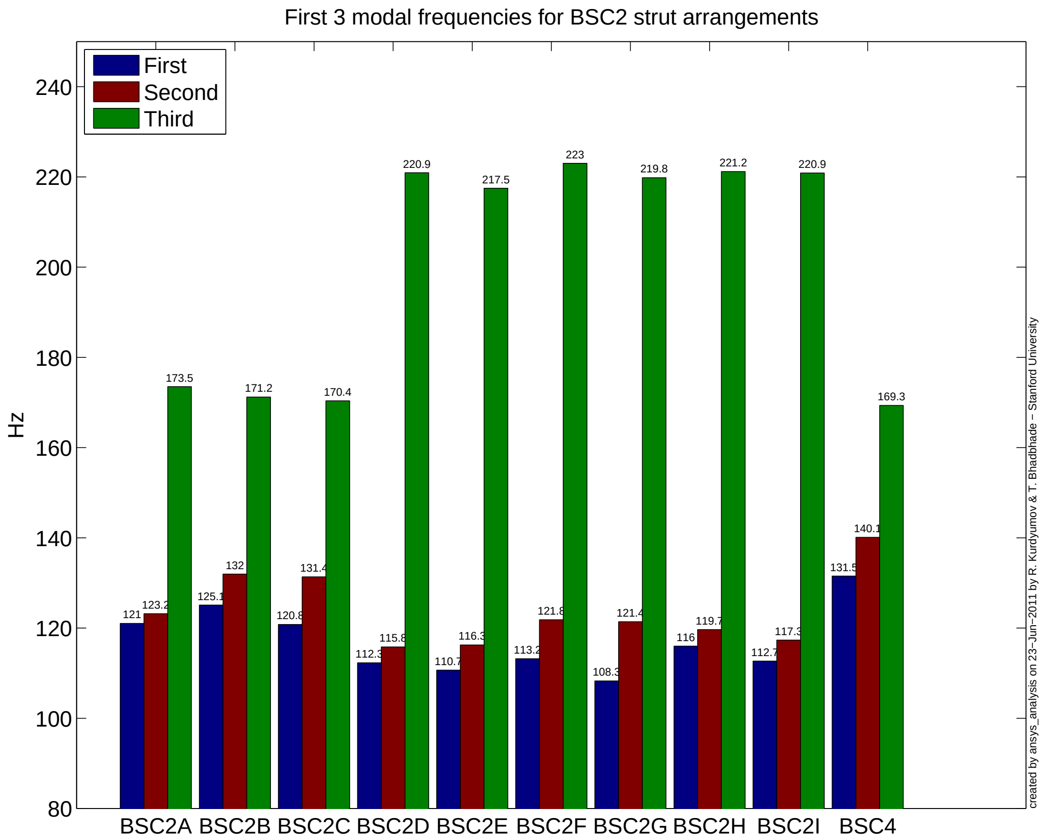

Figure 10: Lowest three modal frequencies for BSC2 strut arrangements. A, B, and C have the best BSC2 modal behavior. The medium extended arrangement for BSC4 is 6 Hz better than any other arrangement.

Using the ANSYS modal analysis, we found the lowest three modal frequencies for each strut arrangement, shown in Figure 10. BSC2A, BSC2B, BSC2C and BSC4 have the best modal behavior. Note that BSC4 has a 1st mode that is 6 Hz higher and a 2nd mode that is 8 Hz higher than the next best strut arrangement.

In the next two subsections, we present the effective modal masses. For the full results, including modal masses for each DOF, as well as cumulative mass fractions, see the Appendix.

4.1 Translational Modal Mass Results

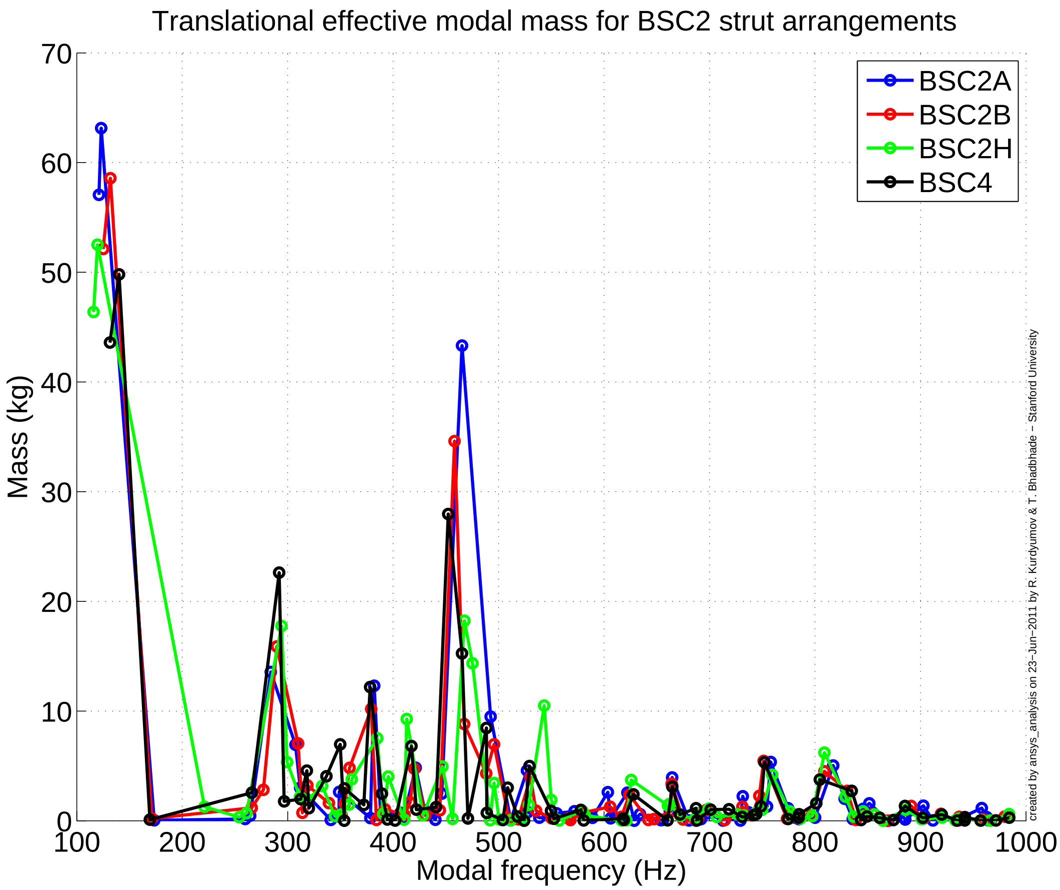

Figure 11: Translational effective mass for each mode (selected BSC2 strut arrangements). BSC4 has the best modal mass. BSC2A and BSC2B had superior modal frequencies, but have higher modal masses than the nominal 'rowboat' configuration BSC2H.

The translational effective masses are shown in Figure 11. BSC2A, BSC2B, and BSC4 were included since these had the best modal frequencies. We also include BSC2H, the 'rowboat' arrangement with medium struts, for comparison. As in BSC7, the first two modes, longitudinal and lateral, have the highest modal mass. This modal mass is substantial, since it's about half of the structure's overall mass (around 118 kg). BSC4 has the lowest modal mass of the three selected arrangements. BSC2H has lower modal mass than the two optimal BSC2 arrangements, but this is offset by first and second modes that are 5 Hz and 12 Hz lower, respectively (see Figure 10). However, BSC2H has a higher modal mass for the 300 Hz mode.

Additionally, the mode below 500 Hz, caused by our fixed support choice, is even more pronounced.

4.2 Rotational Modal Mass Results

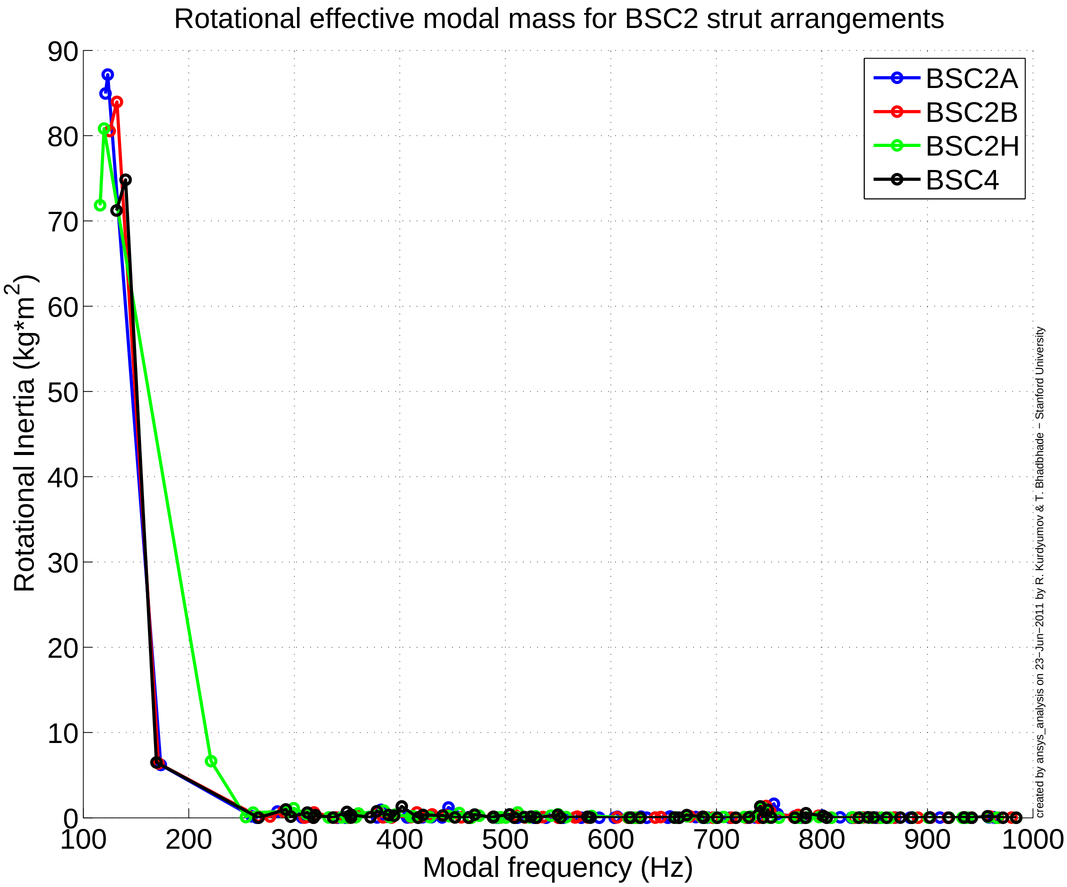

Figure 12: Rotational effective mass for each mode (selected BSC2 strut arrangements). BSC4 has the best modal mass. Again, BSC2A and BSC2B have higher modal masses than the 'rowboat' configuration BSC2H.

The rotational effective masses are shown in Figure 12. The first three modes capture all of the significant rotation of the structure. Again, BSC4 has the best modal mass, and BSC2H, the 'rowboat' configuration, is superior to BSC2A and BSC2B.

4.3 Summary

Based on the analysis, we recommend the BSC2B strut arrangement, since this arrangements has the highest first two modal frequencies, as well as lower modal mass for the 300 Hz mode. However, a case can also be made for BSC2H, the 'rowboat' configuration, since this design has a lower translational and rotational modal mass for the two lowest modes.

BSC4 has the best modal frequencies and modal mass performance, so we recommend that design for the chamber.

For figures that demonstrate the clearance of BSC2B and BSC4, see the Appendix.

5 Varying Fixed Supports

We wanted to examine whether some of the higher frequency (>200 Hz), high modal mass modes calculated by ANSYS were caused by the support conditions - only fixing four short edges on the bottom of the structure. We suspected this was a problem because the base of the structure was moving for each of these high frequency modes, as in Figure 15. To test this, we took the best candidate for BSC2, BSC2B, which has an extended strut arrangement with 2 small, 2 medium struts. We also wanted to check whether overconstraining the struts (by fixing the entire bottom face of the table interface) had an effect on modal behavior. The following cases were tested:

- BSC2FixA: 4 short edges fixed on the bottom of the structure (as in Figure 2), 4 strut faces fixed (nominal BSC2B arrangement)
- BSC2FixB: All outside edges fixed on the bottom of the structure, 4 strut faces fixed
- BSC2FixC: All outside edges fixed on the bottom of the structure, outside edges fixed on each strut
- BSC2FixD: 4 short edges fixed on the bottom of the structure, outside edges fixed on each strut

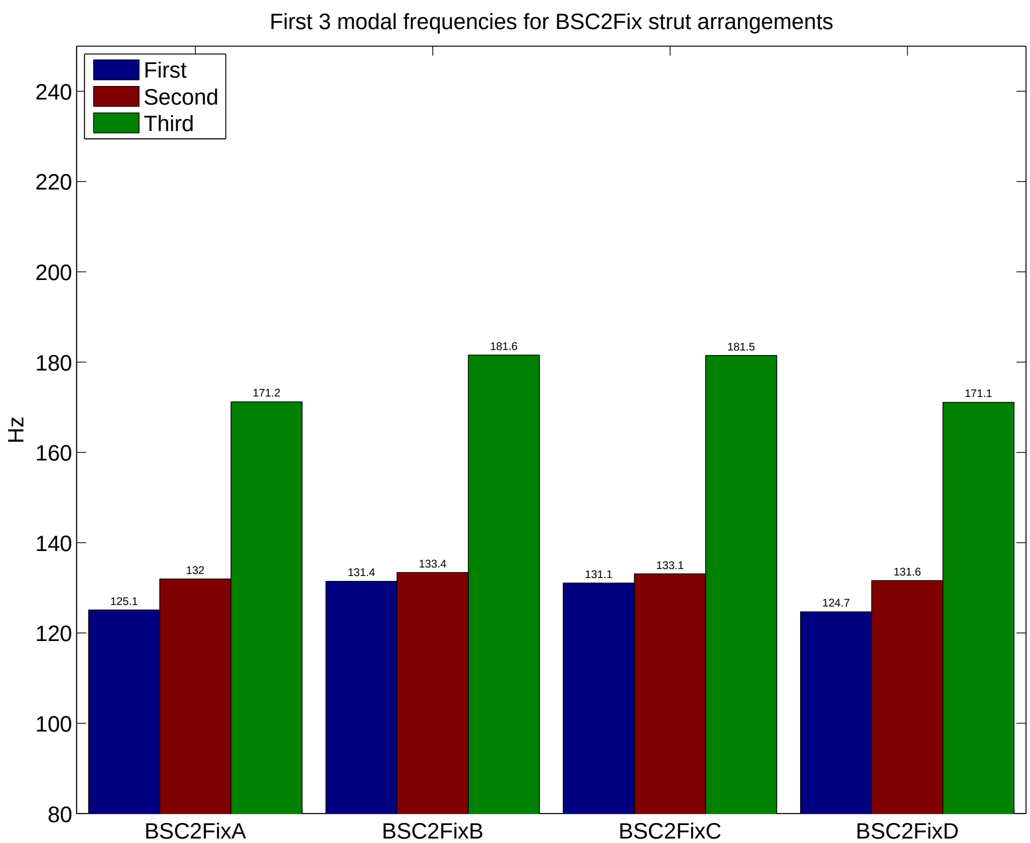

Figure 13: Lowest three modal frequencies for variations on BSC2B with different fixed supports. Fixing the outside edges of the structural base (BSC2FixA→BSC2FixB) significantly increased the 1st and 3rd modal frequencies. Fixing the bottom of the struts along the outside edges rather than attaching the entire base to the optics table (BSC2FixA→ BSC2FixD, BSC2FixB→BSC2FixC) did not have a significant effect.

The lowest three modal frequencies for each of these arrangements are shown in Figure 13. Fixing the structural base caused a large jump in the first (7-8 Hz) and third (10 Hz) modal frequencies. However, the second modal frequency only increased slightly (1 Hz). Fixing the struts along the outside edges, instead of the full bottom face, did not have a significant effect.

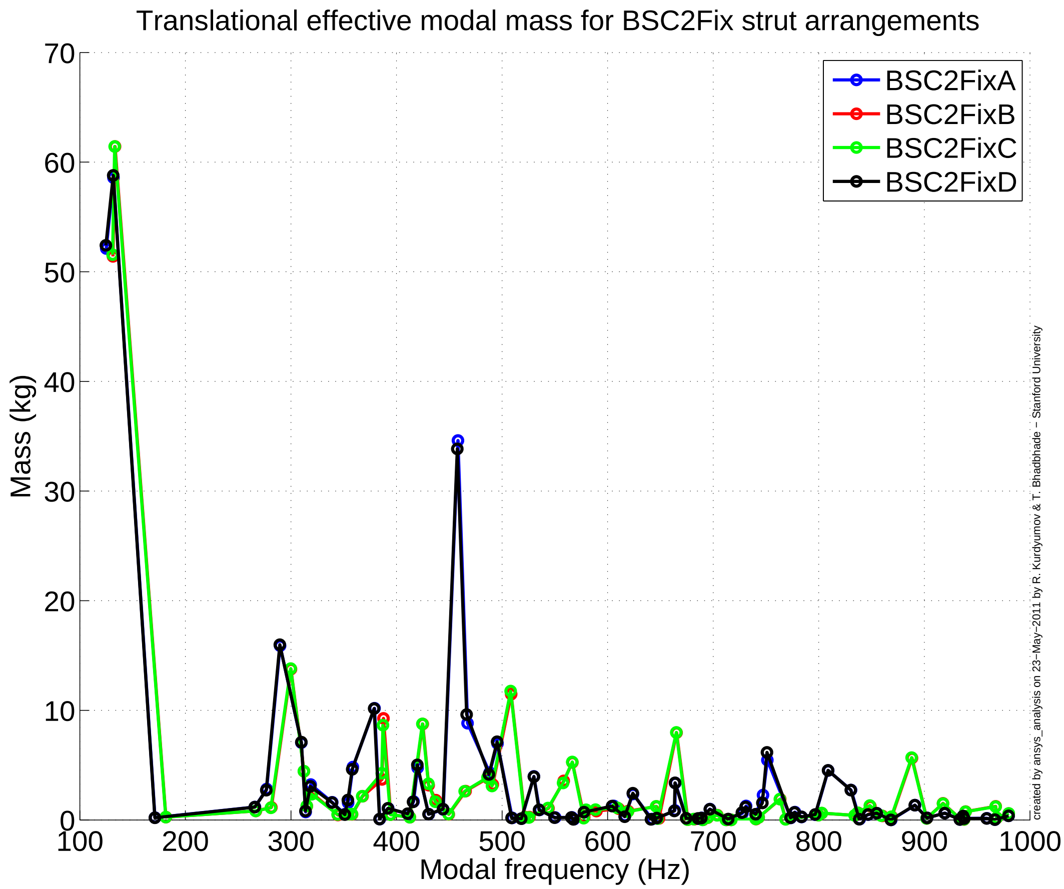

Figure 14: Fixing the structural base outside edges moves the ∼500 Hz mode up in frequency and drastically reduces the modal mass. Some higher frequency modes are also eliminated, but new high frequency modes appear as well. Modes inherent to the structural design (first three and ∼ 300Hz mode) are not significantly affected.

To check which high frequency modes were caused by our fixed supports, we examined the translational and rotational effective modal masses for the above cases. The 458 Hz mode from BSC2B goes from a modal mass of 35 kg to 12 kg with the fixed outside edge structural base (it also shifts up to around 509 Hz). Moreover, the modes that are inherent to the structure (first three and the mode just below 300 Hz) are relatively unaffected by the new fixed support. Also, the two modes above 700 Hz have been eliminated, although other high frequency modes have appeared.

Again, changing the strut fixed supports did not have a signficant effect.

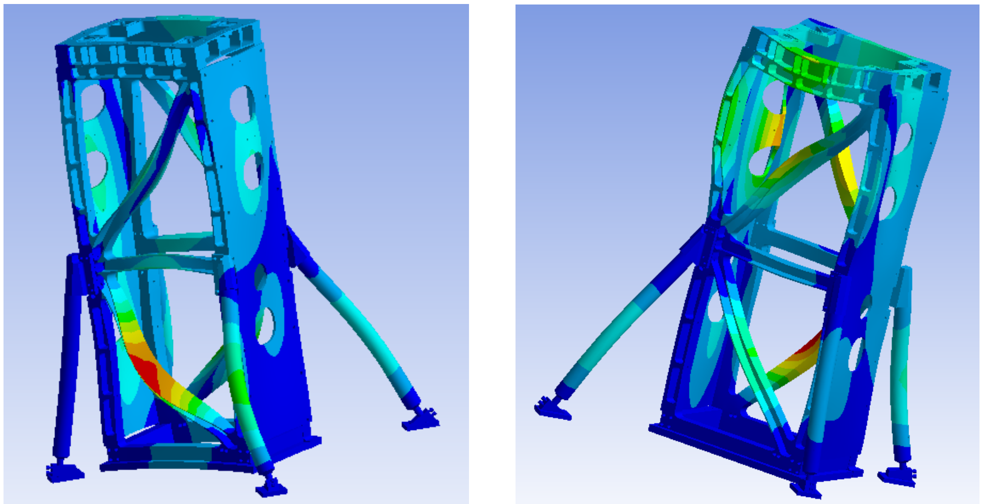

(a) 458Hz (BSC2FixA) **(b)** 509Hz (BSC2FixB)

Figure 15: Difference in deformation of ∼500 Hz mode with the some structural base outside edges fixed (left) and all fixed (right). The original mode has visible structural base motion, while the more firmly fixed structural base on the right leads to a sharp decrease in modal mass because vertical structural motion is much more constrained.

Visually, the difference between the 458 Hz and more strictly fixed 508 Hz mode can be seen in Figure 15. Clearly the structural base is more constrained (it has turned solid blue). As a result, vertical motion of the structure is much more constrained, leading to a reduced modal mass. See Figure 45 in the Appendix for a comparison of vertical (y-direction) effective mass caused by different fixed supports and confirmation that the vertical modal mass has decreased.

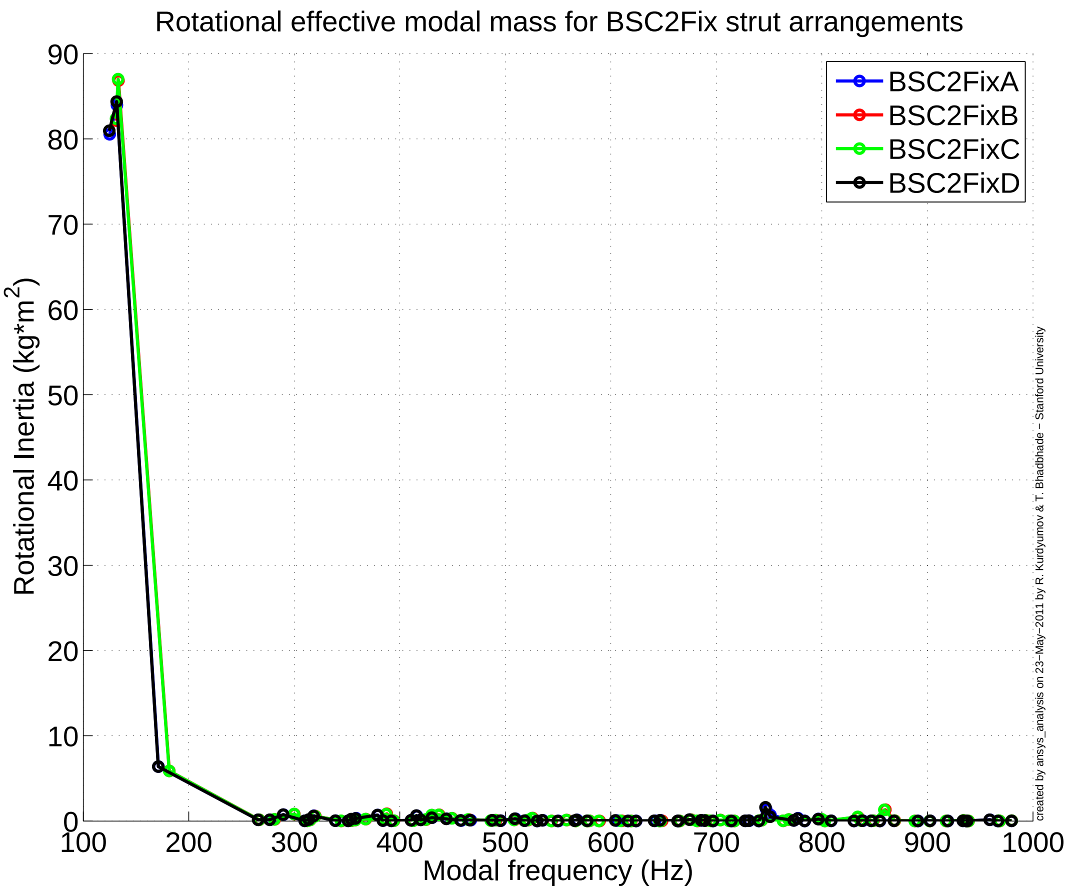

Figure 16: Fixing the structural base outside edges doesn't have a significant effect on rotational modal mass since the first three modes largely determine the modal behavior.

The rotational modal behavior is not affected by the fixed support conditions. The first three modes still account for almost all the modal behavior, and these are inherent to the structural design.

5.1 Summary

We have confirmed that the large ∼500 Hz mode and some of the higher frequency modes were caused by an insufficient number of fixed supports on the structural base in our simulation. Adding constraints, more representative of the dog clamping used on the actual structure, signficantly reduced the modal mass of these modes. Properly contraining the base of the structure allows us to focus on the lowest 3 modes, as well as the ∼300 Hz mode.

6 Conclusions

Using FEA modal analysis, we have determined the optimal strut arrangements for BSC2, BSC4, BSC7, and BSC8, and re-emphasized the importance of good clamping. In choosing optimal strut arrangements, we have chosen to minimize modal mass and maximize modal frequency for the lowest two structural modes. Other important factors include the frequency of the third structural mode, and the modal mass of higher frequency modes, particularly the 300 Hz mode.

The optimal strut arrangement for BSC7 and BSC8, the most space constrained of the chambers, has two short extended struts, one medium extended strut, and one medium inward strut (BSC7B). This configuration has a much higher second modal frequency and modal masses that are at least 10% lower than the next best arrangement. Another arrangement (BSC7E) had a slightly higher first modal frequency (by 2Hz), but this was outweighed by the significant decrease in the frequency of the second mode.

The optimal strut arrangement for BSC2 has 4 extended struts, two short and two medium (BSC2B). This arrangement has first and second modes that are 5 Hz and 12 Hz higher, respectively, than the 'rowboat' arrangement (BSC2H). The 'rowboat' arrangement also has a higher 300 Hz mode modal mass. However, a case can be made for the 'rowboat' arrangement since its modal masses are $\sim 10\%$ lower.

The best strut arrangement found could only fit into BSC4 - 4 extended medium struts. This arrangement has first and second modes that are 15 Hz and 20 Hz higher, respectively, than the 'rowboat' arrangement. It also has slightly lower modal mass than the 'rowboat' arrangement. The only drawback is that it has the highest modal mass for the 300 Hz mode.

Although each modal analysis found up to 70 modes below 1000Hz, most of these modes had negligible modal mass. We did, however, find two significant modes near 300 Hz and 500 Hz. The 300 Hz mode mainly involved motion near the middle of structure, with significant deformation along the single cross-bracing element. The 500 Hz mode was due to loose fixed supports on the structural base (in simulation) causing the structure to move in the vertical direction. This simulated mode was greatly reduced with more firm fixed support conditions.

One of the primary concerns going into the analysis was whether the 'strut modes' of the structure would be a problem. These are modes where the struts are being signficantly deformed, inducing structural modes that would not otherwise exist. We did not find any strut modes with significant modal mass, so this doesn't seem to be a huge problem.

A Appendix

A.1 Side Plate Analysis

We examined the effects of adding access holes to the side plates in the beam splitter. The ANSYS simulations had the following assumptions:

- Modes > 20 Hz
- An 8 kg point mass centered on the top plane of the structure
- Aluminum parts, except stainless steel fixtures and stainless steel stay leg table interfaces
- The side plate rigidly attached across the entire contact surface (note that we did not use patches at each bolt hole)
- The bottom faces of the stay leg table interfaces fixed
- Four short edges of the bottom of the structure fixed, as in Figure 2

To make sure that the results were not biased toward a particular strut arrangement, we analyzed for an extended strut arrangement and a modified extended strut arrangement, shown in Figure 17. The results are presented in Table 1. The side plates used were: nomimal, rectangular, 5" diameter circles, 5" side squares, criss-cross, and 3 straight slots.

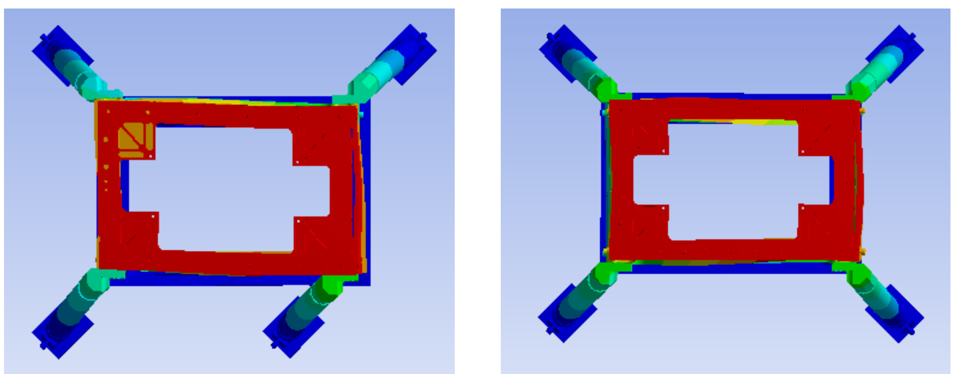

(a) 3 extended struts

(b) 4 extended struts

Figure 17: Strut arrangements used for the side plate FEA analysis.

Strut Arrangement	Holes	1st Mode	Type	2nd Mode	Type	3rd Mode	Type
4 small extended struts	Nominal	120.53	Lat.*	123.97	Long.*	176.41	Tors.
	Rectangles	113.83	Long.	123.94	Lat.	169.76	Tors.
	Circles	121.29	Long.	122.52	Lat.	174.35	Tors.
	Squares	119.80	Long.	122.64	Lat.	172.85	Tors.
	Criss-cross	118.84	Long.	126.11	Lat.	179.81	Tors.
	Slots	120.23	Long.	122.77	Lat.	172.95	Tors.
3 small extended struts	Nominal	109.69	Lat.*	127.71	Long.*	189.06	Tors.
	Rectangles	107.19	Long.*	123.57	Lat.*	180.81	Tors.
	Circles	109.83	Lat.*	126.83	Long.*	187.12	Tors.

Table 1: Side plate FEA results. Modes are listed in Hz. The plate with circular holes actually moved the 1st modal frequency up compared to the nominal plate. We didn't analyze all the designs for the 3 extended struts since the first three designs confirmed there was no strut arrangement bias. The starred (*) entries had substantial diagonal motion.

Based on the results, we recommended the circular access holes. They provided an upward shift in the lowest mode in both strut arrangements, and minimal changes to the other two primary modes. However, the slotted arrangement was ultimately chosen since it gave improved access to the beam splitter during mechanical assembly.

A.2 Clearance Verification

To guarantee that the BSC2B and BSC4 strut arrangements will fit in the chambers, we performed clearance verification. Since BSC7B already falls within the space of the previous strut arrangement, the clearance verification is not needed. For BSC2B, we have approximately 0.82" of clearance between a small strut and the structural beam member (D972121-1). The clearance is shown in Figure 18.

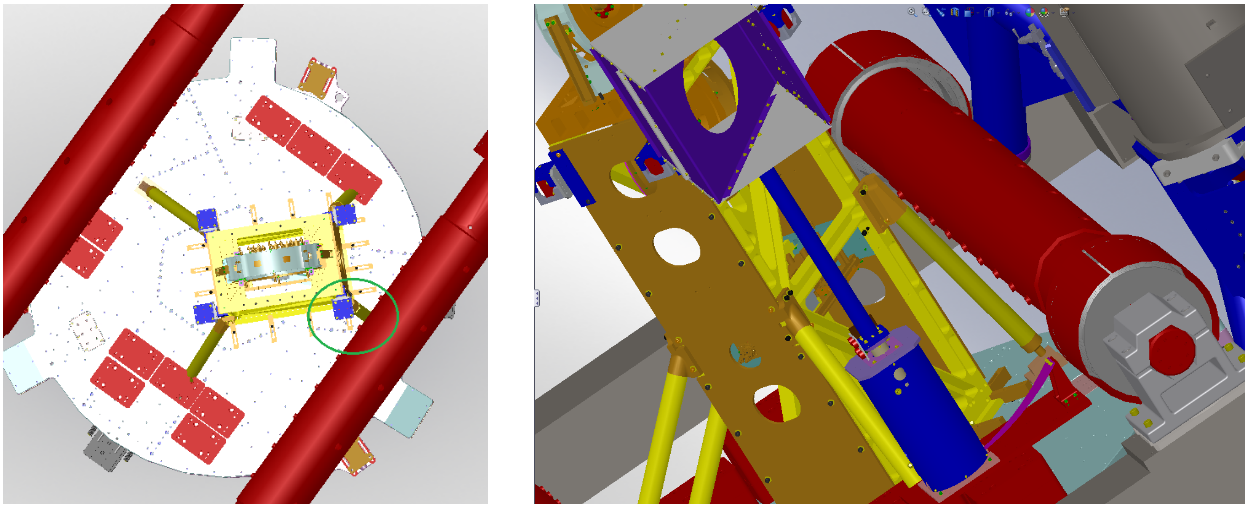

(a) **(b)**

Figure 18: Clearance verification for BSC2B. There is 0.82" of clearance between the short strut and the structural beam member.

For BSC4, we have approximately 1.2" of clearance between a medium strut and the structural beam member, as shown in Figure 19.

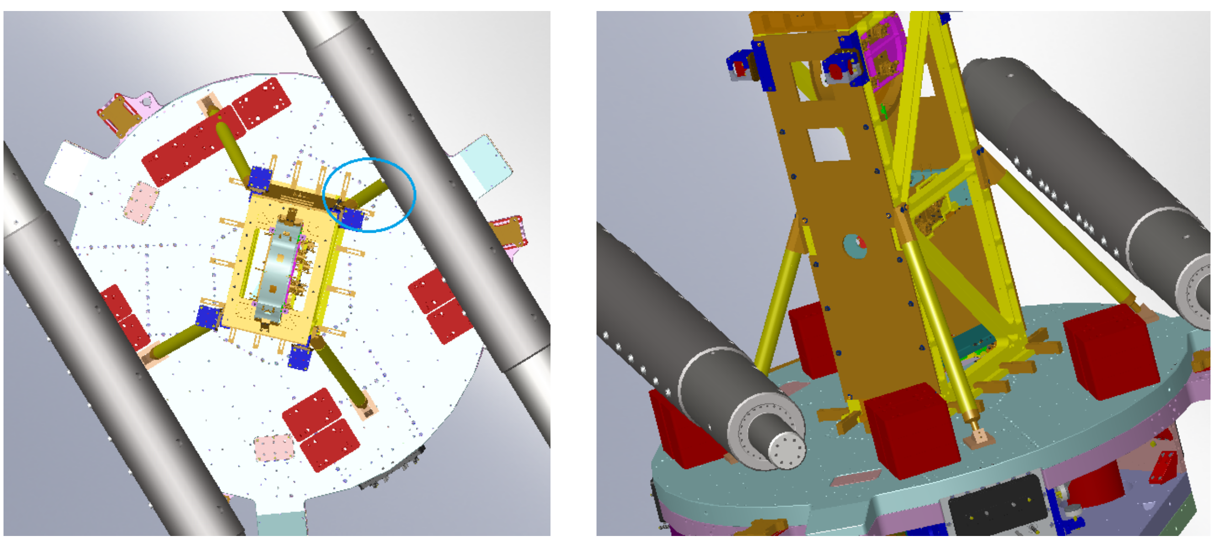

(a) **(b)**

Figure 19: Clearance verification for BSC4. There is 1.2" of clearance between the medium strut and the structural beam member.

A.3 BSC7 Full Results

The following three sections include the full results reported by ANSYS for select strut arrangements. We include plots of the effective mass in each degree of freedom. These effective masses were combined using quadrature scaling, as described earlier in the report.

We also include the cumulative mass fraction in each degree of freedom. The CMF provides an indication of what frequency range captures most of the modal behavior of our structure. ANSYS defines it as the running sum of the effective mass over the total effective mass (up to the max frequency searched). We consider a CMF above 90% to be a good indicator that we have captured modal behavior up to our max frequency searched [1].

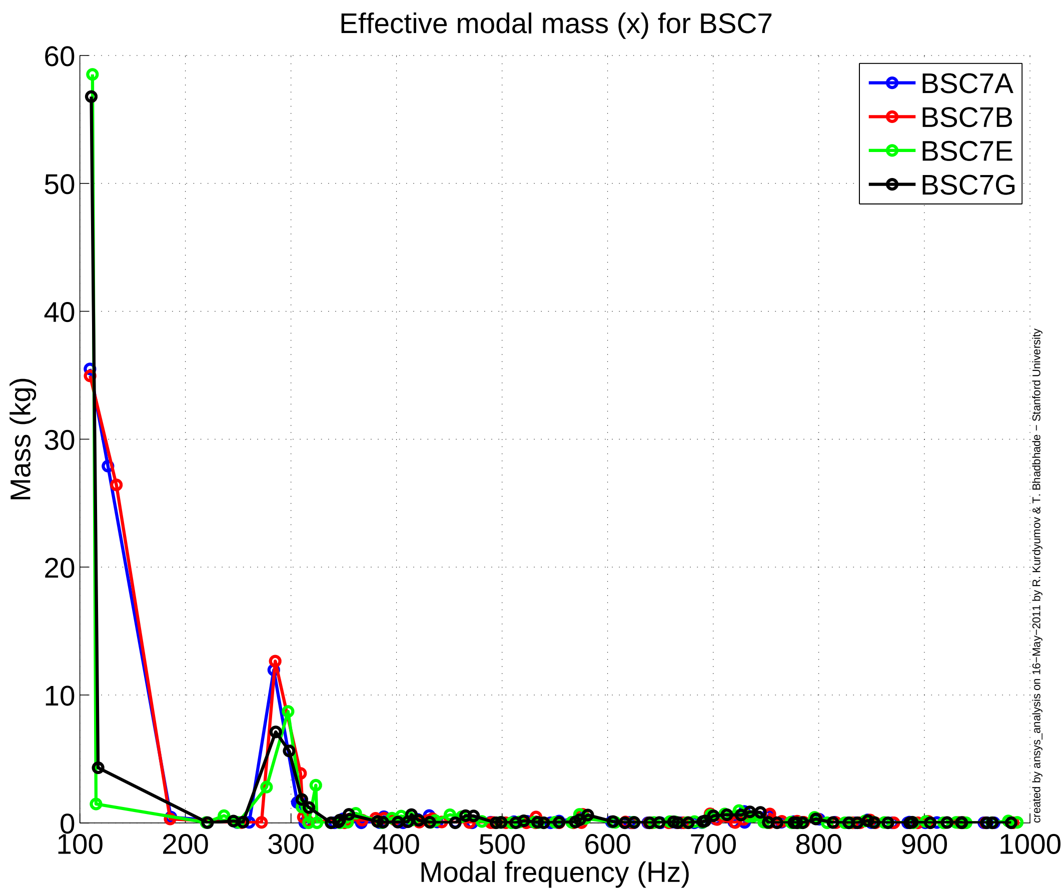

Figure 20

[1]On a semi-related note, in modal analysis, we usually judge our model by its total effective modal mass compared to the actual mass. If the ratio is above 90%, we have a pretty good model.

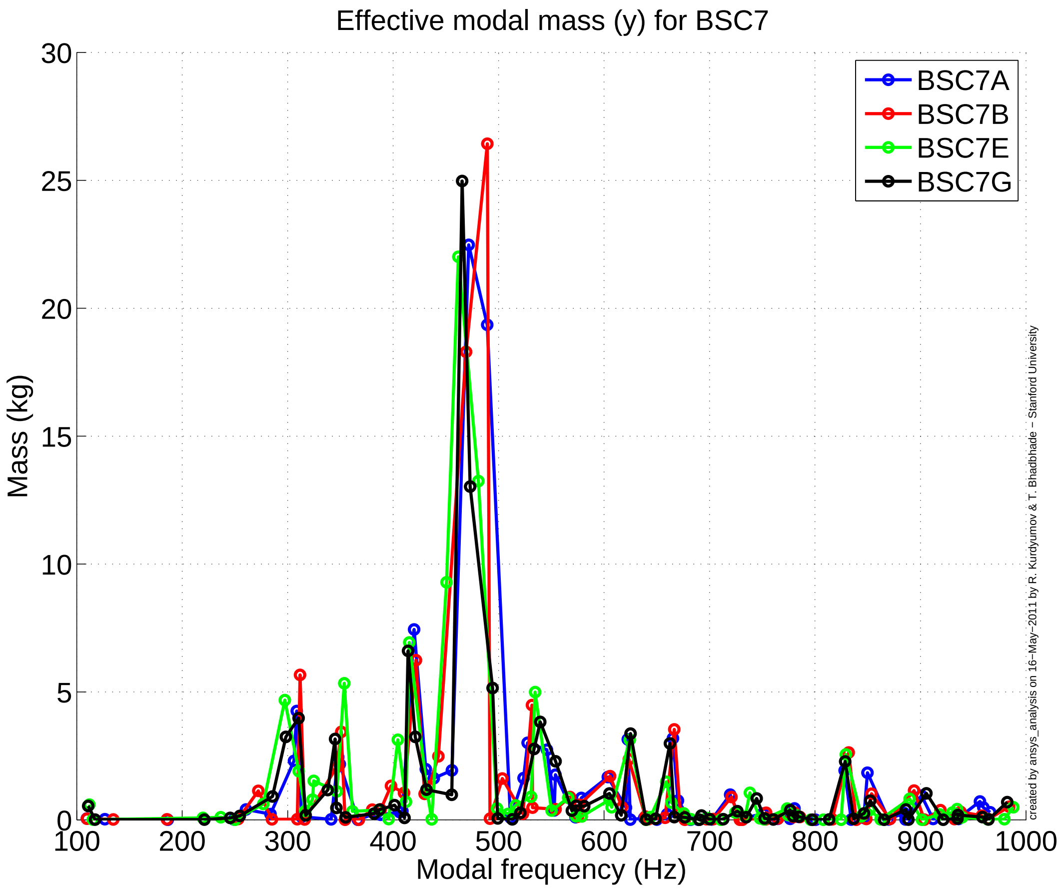
Effective modal mass (y) for BSC7
Mass (kg)
Modal frequency (Hz)
0
5
10
15
20
25
30
100
200
300
400
500
600
700
800
900
1000
BSC7A
BSC7B
BSC7E
BSC7G
created by ansys_analysis on 16−May−2011 by R. Kurdyumov & T. Bhadbhade − Stanford University

Figure 21

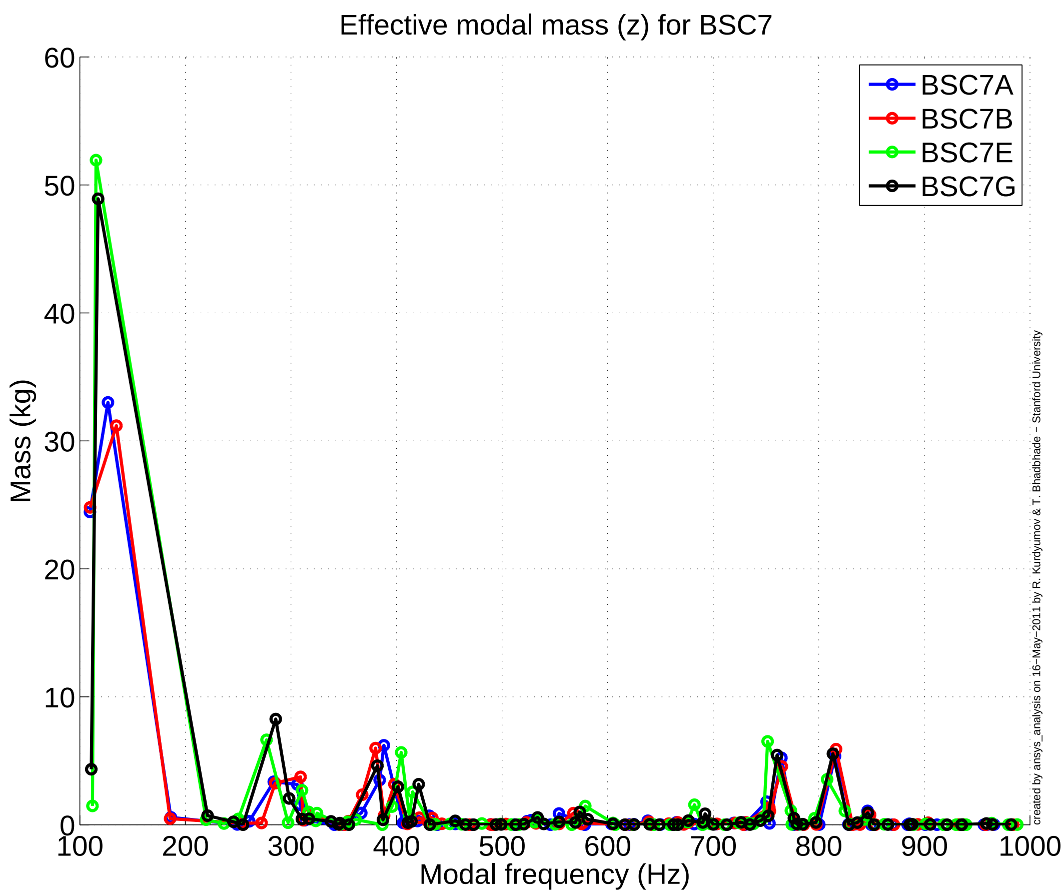

Effective modal mass (z) for BSC7
Mass (kg)
Modal frequency (Hz)
BSC7A
BSC7B
BSC7E
BSC7G
0
10
20
30
40
50
60
100
200
300
400
500
600
700
800
900
1000
created by ansys_analysis on 16−May−2011 by R. Kurdyumov & T. Bhadbhade − Stanford University

Figure 22

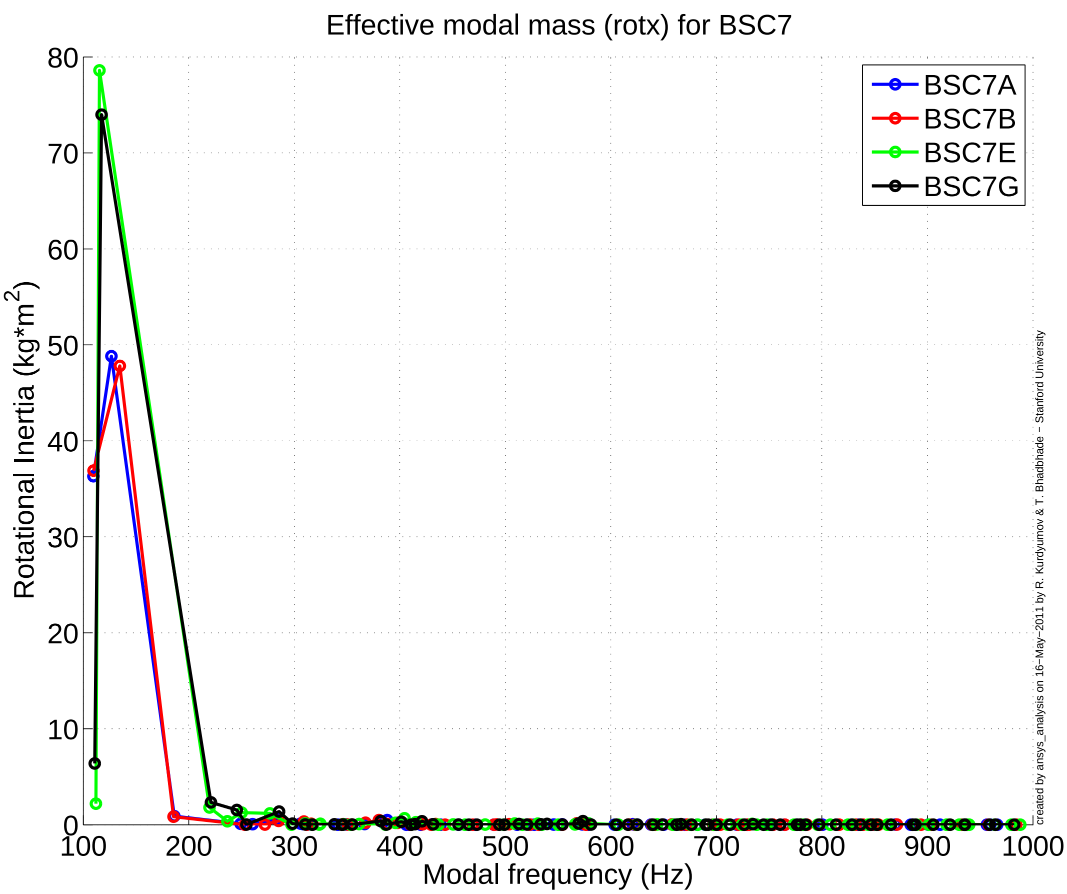

Effective modal mass (rotx) for BSC7
Rotational Inertia (kg*m^2)
Modal frequency (Hz)
BSC7A
BSC7B
BSC7E
BSC7G
0
10
20
30
40
50
60
70
80
100
200
300
400
500
600
700
800
900
1000
created by ansys_analysis on 16−May−2011 by R. Kurdyumov & T. Bhadbhade − Stanford University

Figure 23

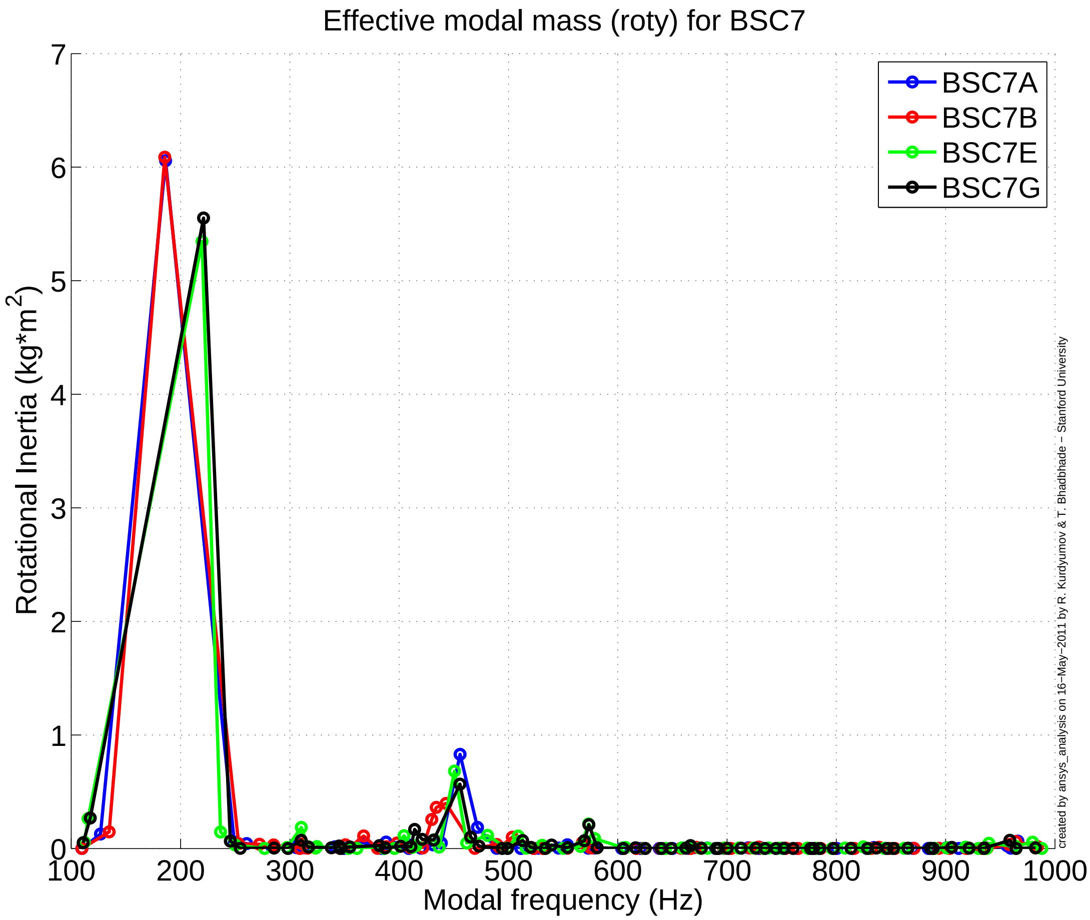

Effective modal mass (roty) for BSC7
Rotational Inertia (kg*m^2)
Modal frequency (Hz)
BSC7A
BSC7B
BSC7E
BSC7G
0
1
2
3
4
5
6
7
100
200
300
400
500
600
700
800
900
1000
created by ansys_analysis on 16−May−2011 by R. Kurdyumov & T. Bhadbhade − Stanford University

Figure 24

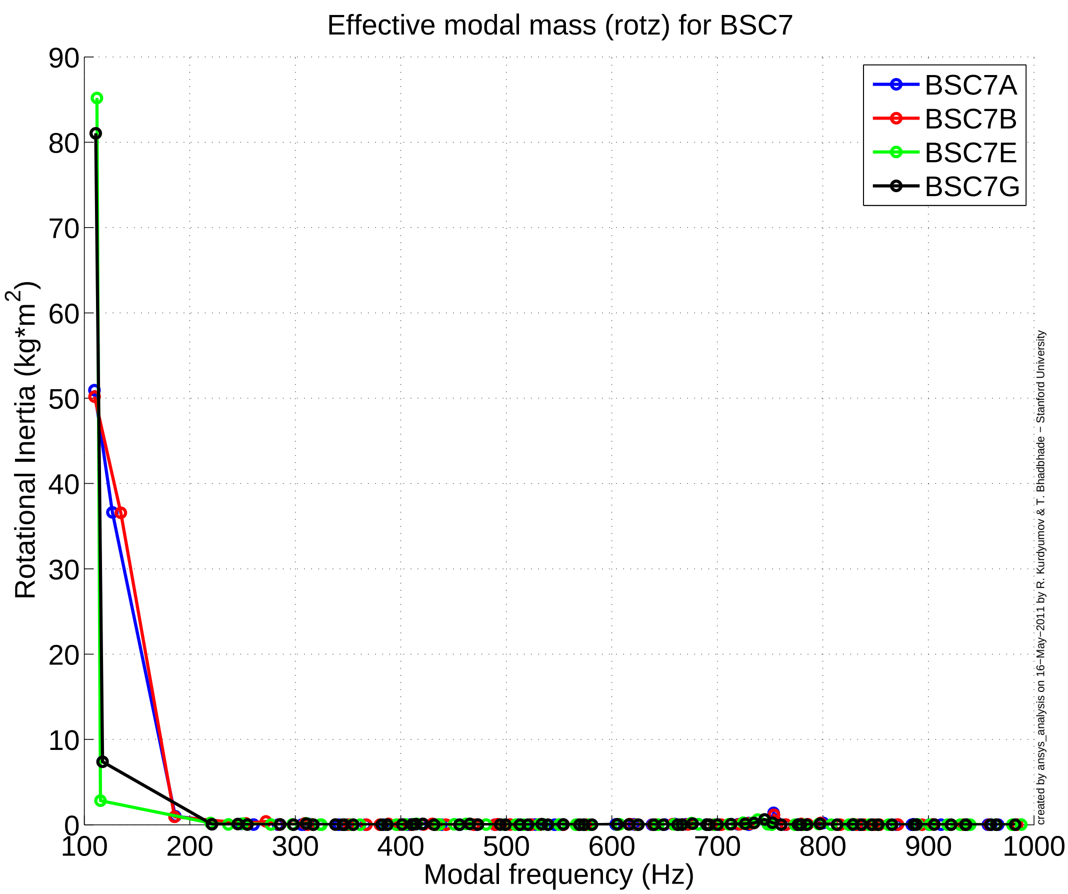

Effective modal mass (rotz) for BSC7
Rotational Inertia (kg*m^2)
Modal frequency (Hz)
BSC7A
BSC7B
BSC7E
BSC7G
0
10
20
30
40
50
60
70
80
90
100
200
300
400
500
600
700
800
900
1000
created by ansys_analysis on 16−May−2011 by R. Kurdyumov & T. Bhadbhade − Stanford University

Figure 25

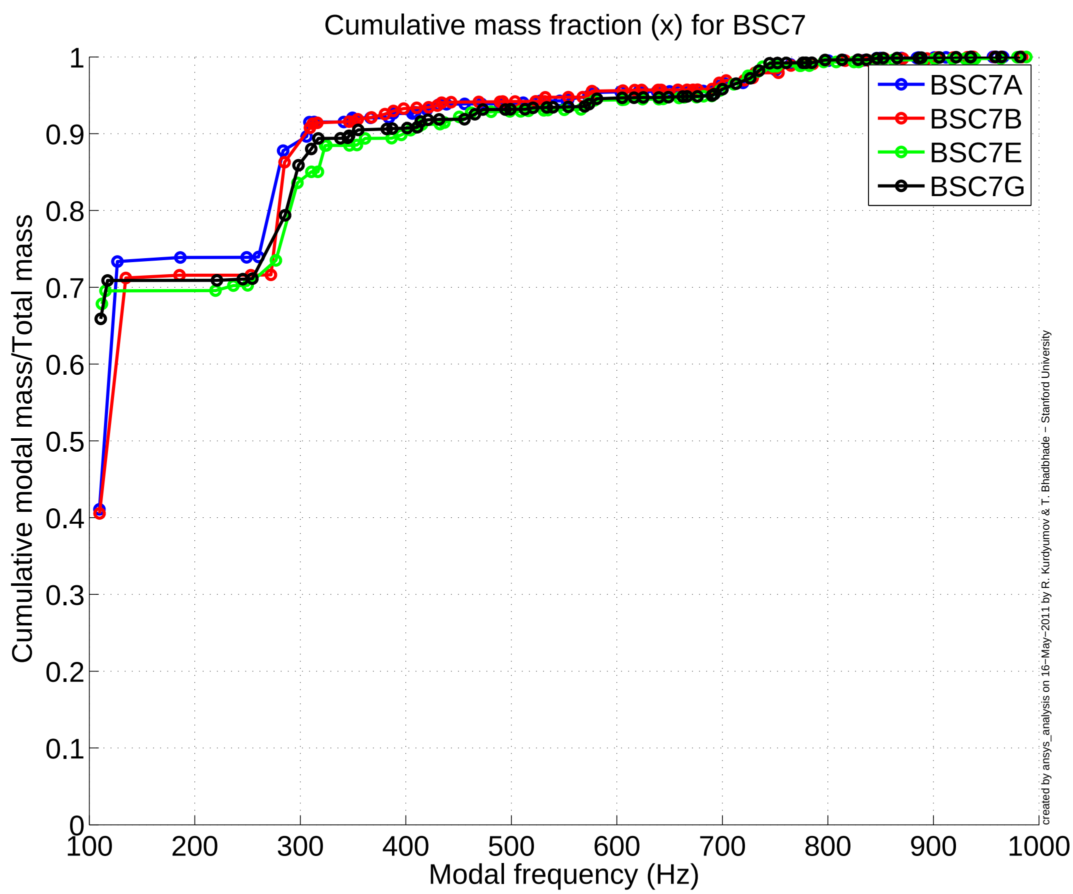

Cumulative mass fraction (x) for BSC7
Cumulative modal mass/Total mass
Modal frequency (Hz)
BSC7A
BSC7B
BSC7E
BSC7G
0
0.1
0.2
0.3
0.4
0.5
0.6
0.7
0.8
0.9
1
100
200
300
400
500
600
700
800
900
1000
created by ansys_analysis on 16−May−2011 by R. Kurdyumov & T. Bhadbhade − Stanford University

Figure 26

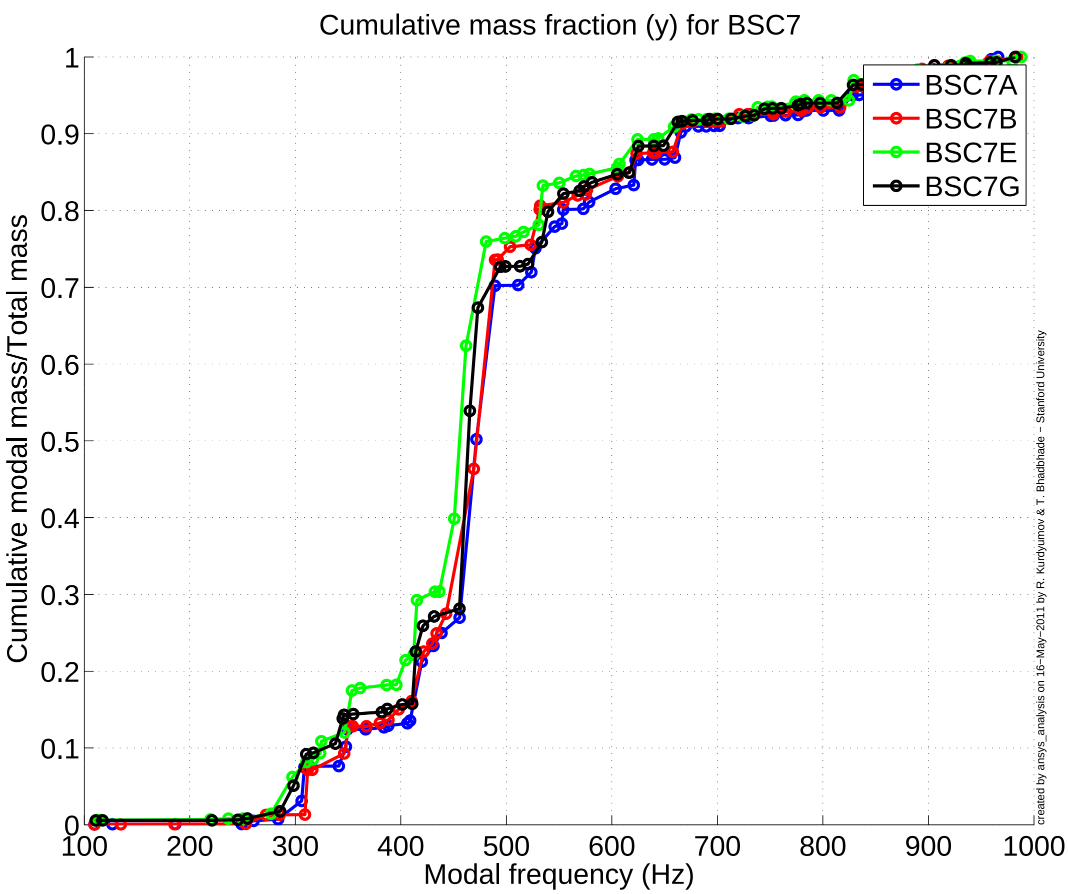

Cumulative mass fraction (y) for BSC7
Cumulative modal mass/Total mass
Modal frequency (Hz)
BSC7A
BSC7B
BSC7E
BSC7G
0
0.1
0.2
0.3
0.4
0.5
0.6
0.7
0.8
0.9
1
100
200
300
400
500
600
700
800
900
1000
created by ansys_analysis on 16−May−2011 by R. Kurdyumov & T. Bhadbhade − Stanford University

Figure 27

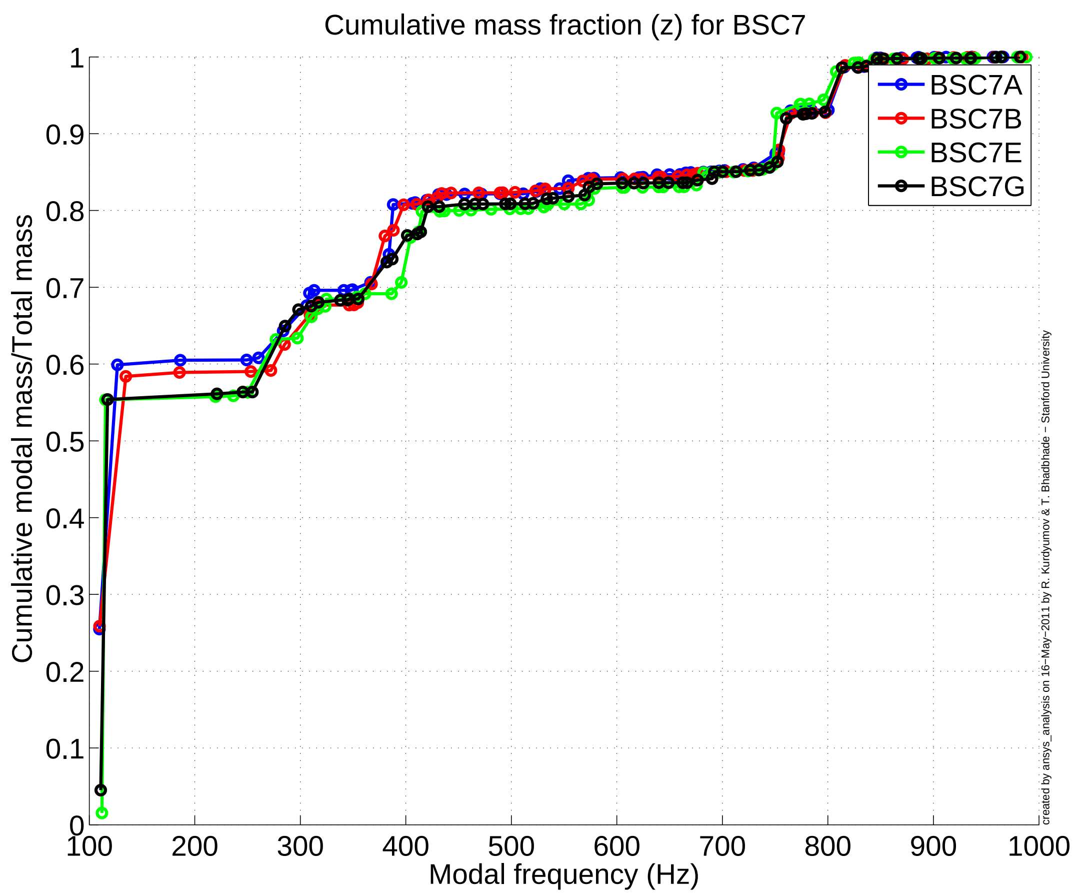
Cumulative mass fraction (z) for BSC7
Cumulative modal mass/Total mass
Modal frequency (Hz)
BSC7A
BSC7B
BSC7E
BSC7G
0
0.1
0.2
0.3
0.4
0.5
0.6
0.7
0.8
0.9
1
100
200
300
400
500
600
700
800
900
1000
created by ansys_analysis on 16−May−2011 by R. Kurdyumov & T. Bhadbhade − Stanford University

Figure 28

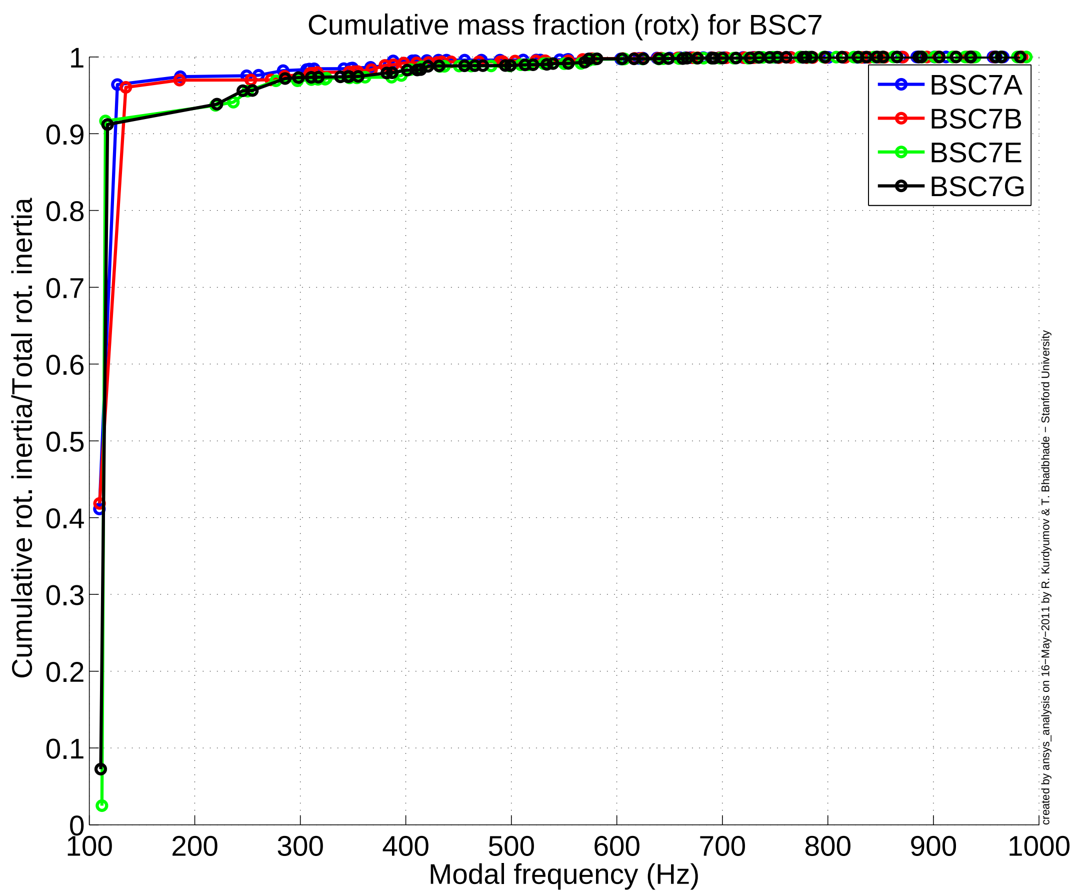

Cumulative mass fraction (rotx) for BSC7
Cumulative rot. inertia/Total rot. inertia
Modal frequency (Hz)
BSC7A
BSC7B
BSC7E
BSC7G
0
0.1
0.2
0.3
0.4
0.5
0.6
0.7
0.8
0.9
1
100
200
300
400
500
600
700
800
900
1000
created by ansys_analysis on 16−May−2011 by R. Kurdyumov & T. Bhadbhade − Stanford University

Figure 29

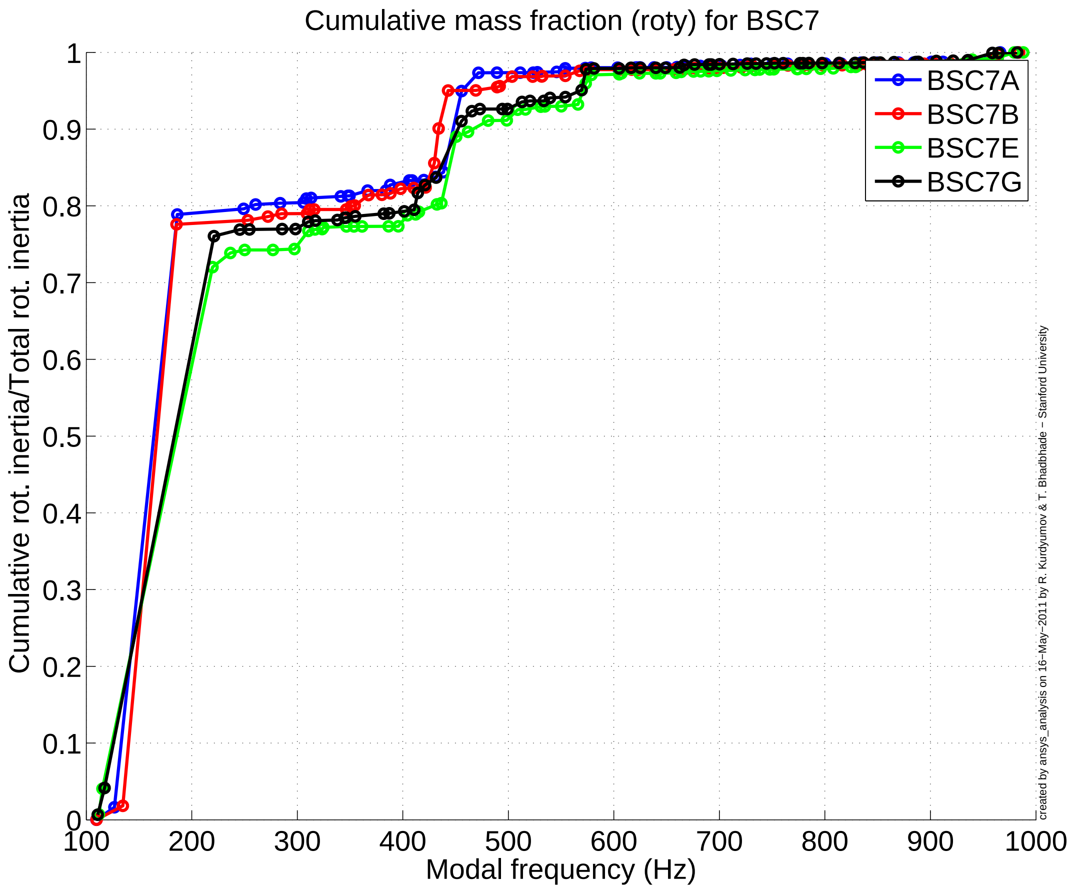
Cumulative mass fraction (roty) for BSC7
Cumulative rot. inertia/Total rot. inertia
Modal frequency (Hz)
BSC7A
BSC7B
BSC7E
BSC7G
0
0.1
0.2
0.3
0.4
0.5
0.6
0.7
0.8
0.9
1
100
200
300
400
500
600
700
800
900
1000
created by ansys_analysis on 16−May−2011 by R. Kurdyumov & T. Bhadbhade − Stanford University

Figure 30

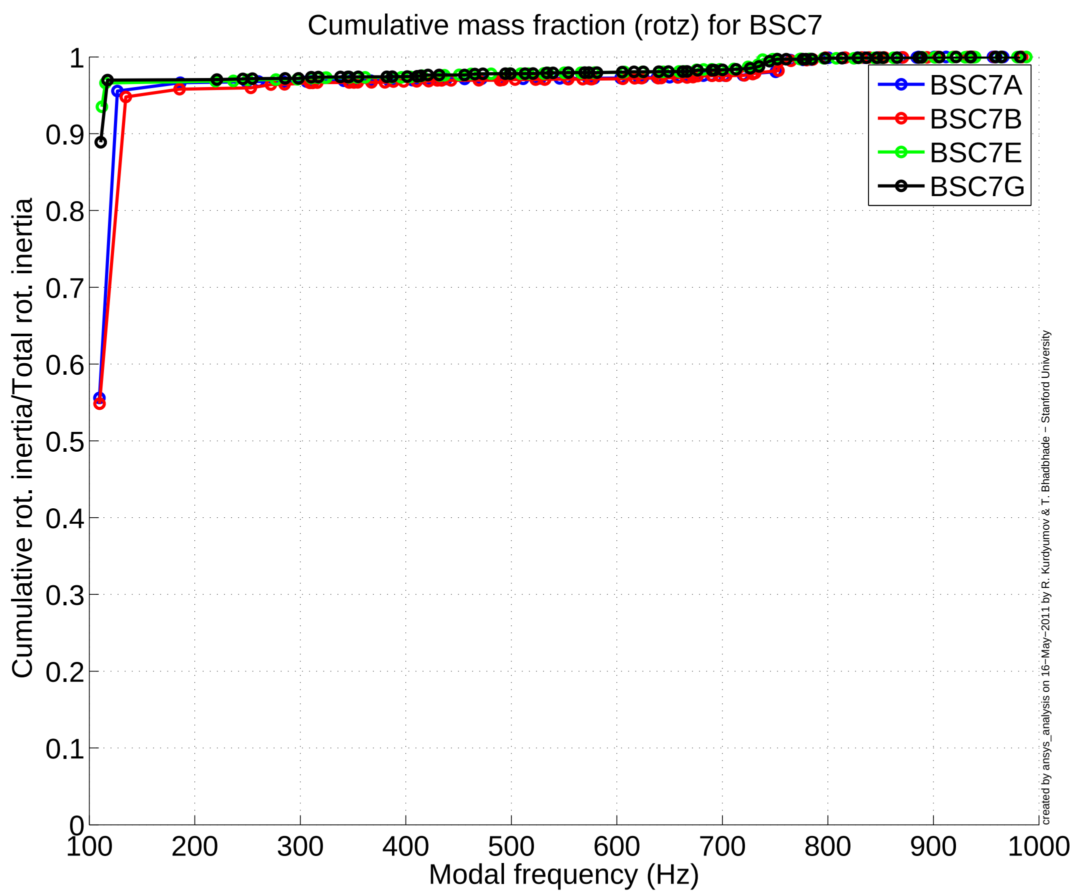
Cumulative mass fraction (rotz) for BSC7
Cumulative rot. inertia/Total rot. inertia
Modal frequency (Hz)
BSC7A
BSC7B
BSC7E
BSC7G
0
0.1
0.2
0.3
0.4
0.5
0.6
0.7
0.8
0.9
1
100
200
300
400
500
600
700
800
900
1000
created by ansys_analysis on 16−May−2011 by R. Kurdyumov & T. Bhadbhade − Stanford University

Figure 31

A.4 BSC2 Full Results

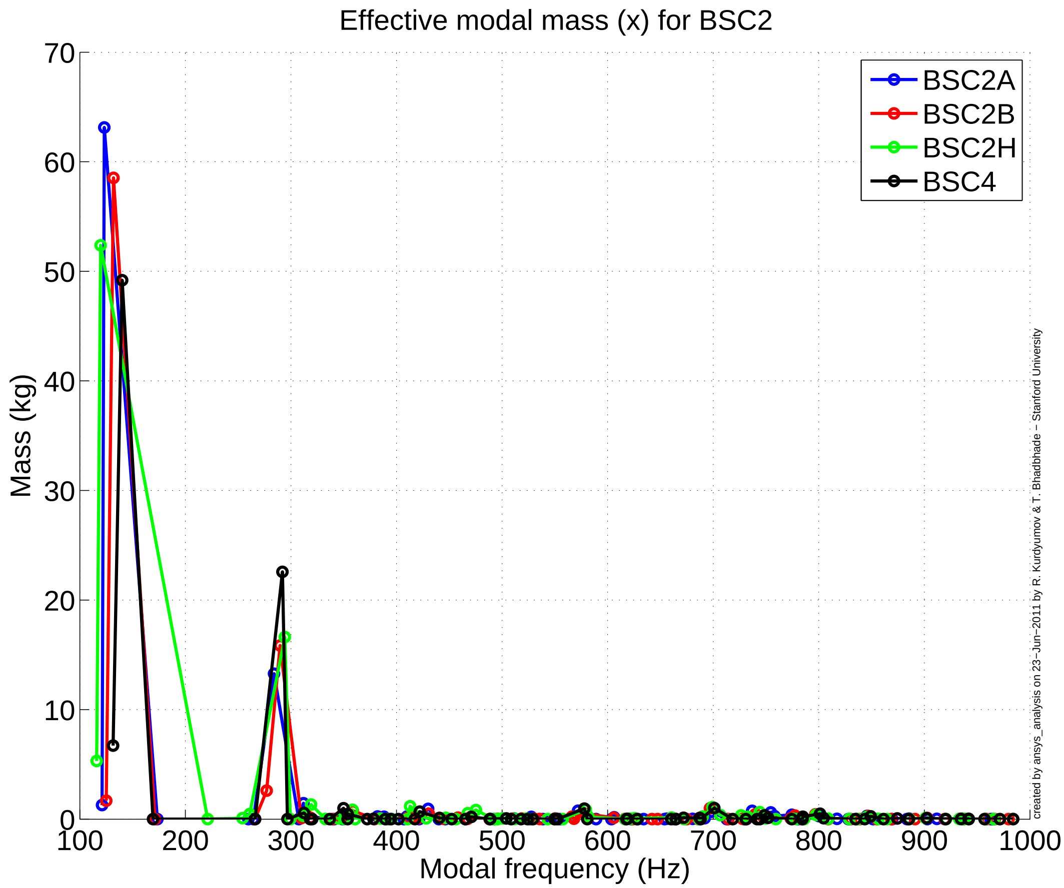

Figure 32

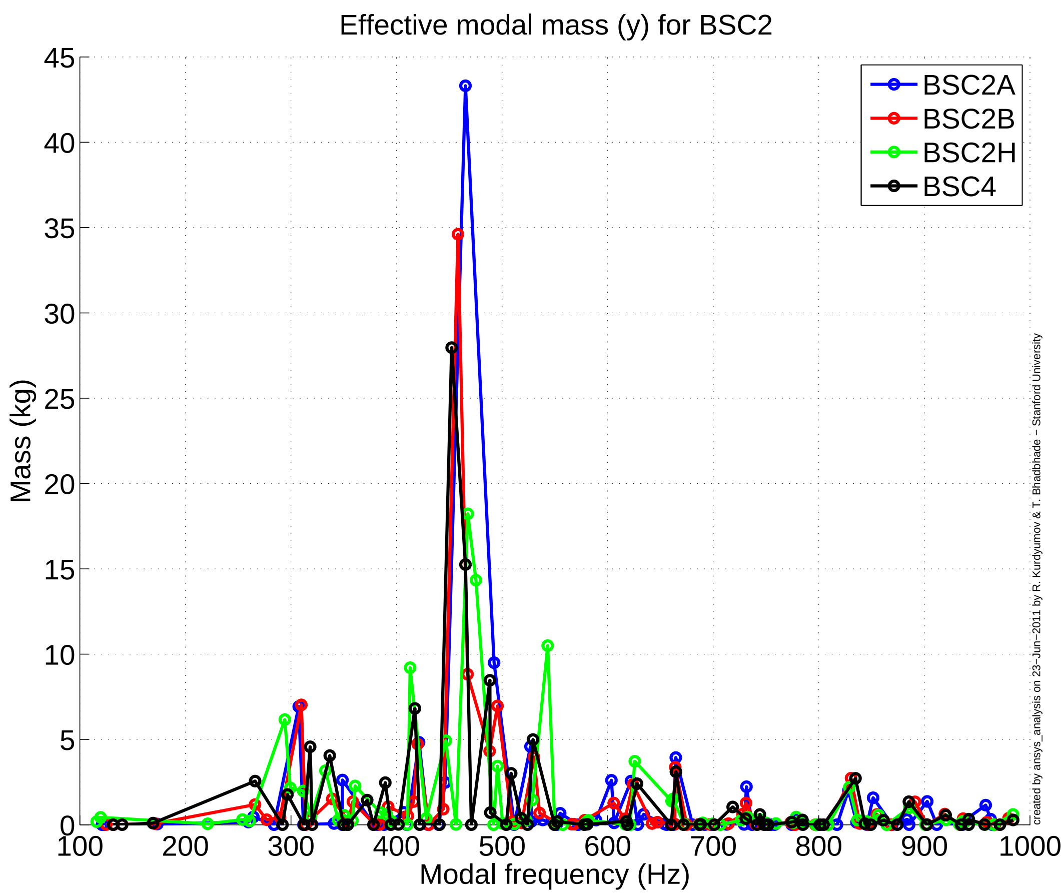
Effective modal mass (y) for BSC2
Mass (kg)
Modal frequency (Hz)
BSC2A
BSC2B
BSC2H
BSC4
created by ansys_analysis on 23−Jun−2011 by R. Kurdyumov & T. Bhadbhade − Stanford University

Figure 33

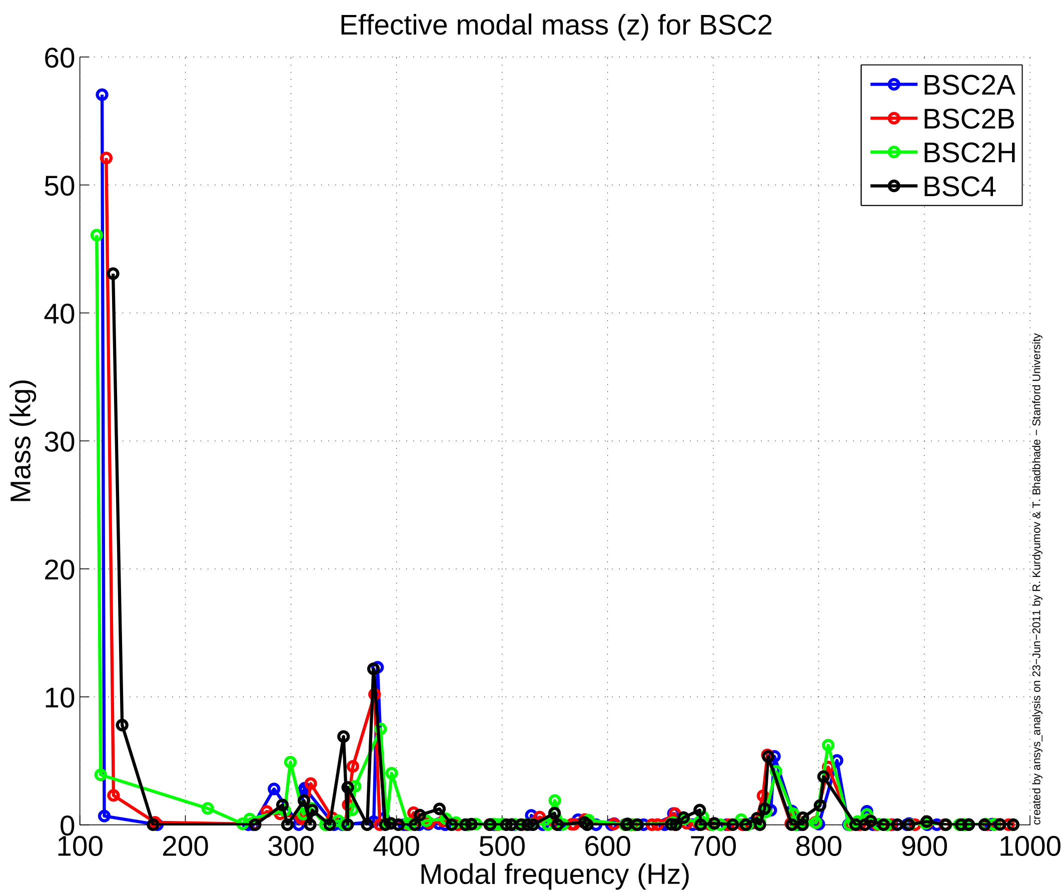
Effective modal mass (z) for BSC2
Mass (kg)
Modal frequency (Hz)
BSC2A
BSC2B
BSC2H
BSC4
0
10
20
30
40
50
60
100
200
300
400
500
600
700
800
900
1000
created by ansys_analysis on 23−Jun−2011 by R. Kurdyumov & T. Bhadbhade − Stanford University

Figure 34

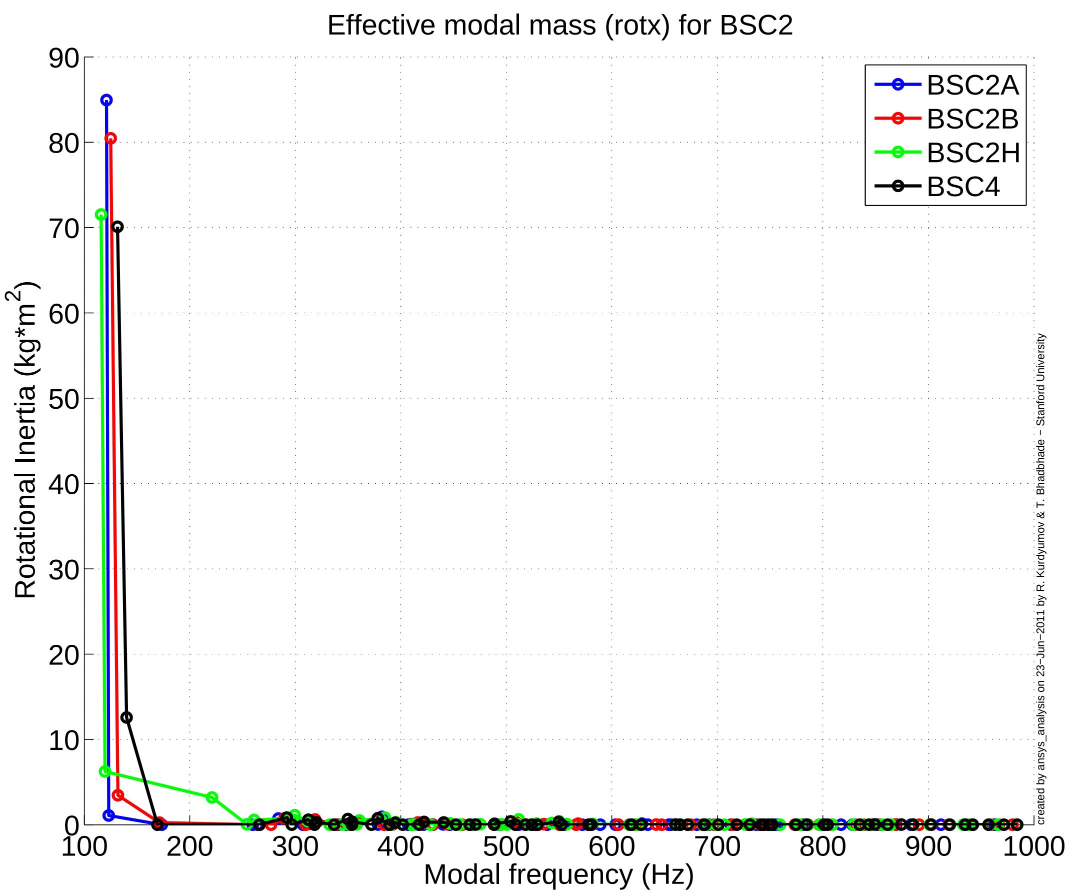
Effective modal mass (rotx) for BSC2
BSC2A
BSC2B
BSC2H
BSC4
Rotational Inertia (kg*m^2)
Modal frequency (Hz)
0
10
20
30
40
50
60
70
80
90
100
200
300
400
500
600
700
800
900
1000
created by ansys_analysis on 23−Jun−2011 by R. Kurdyumov & T. Bhadbhade − Stanford University

Figure 35

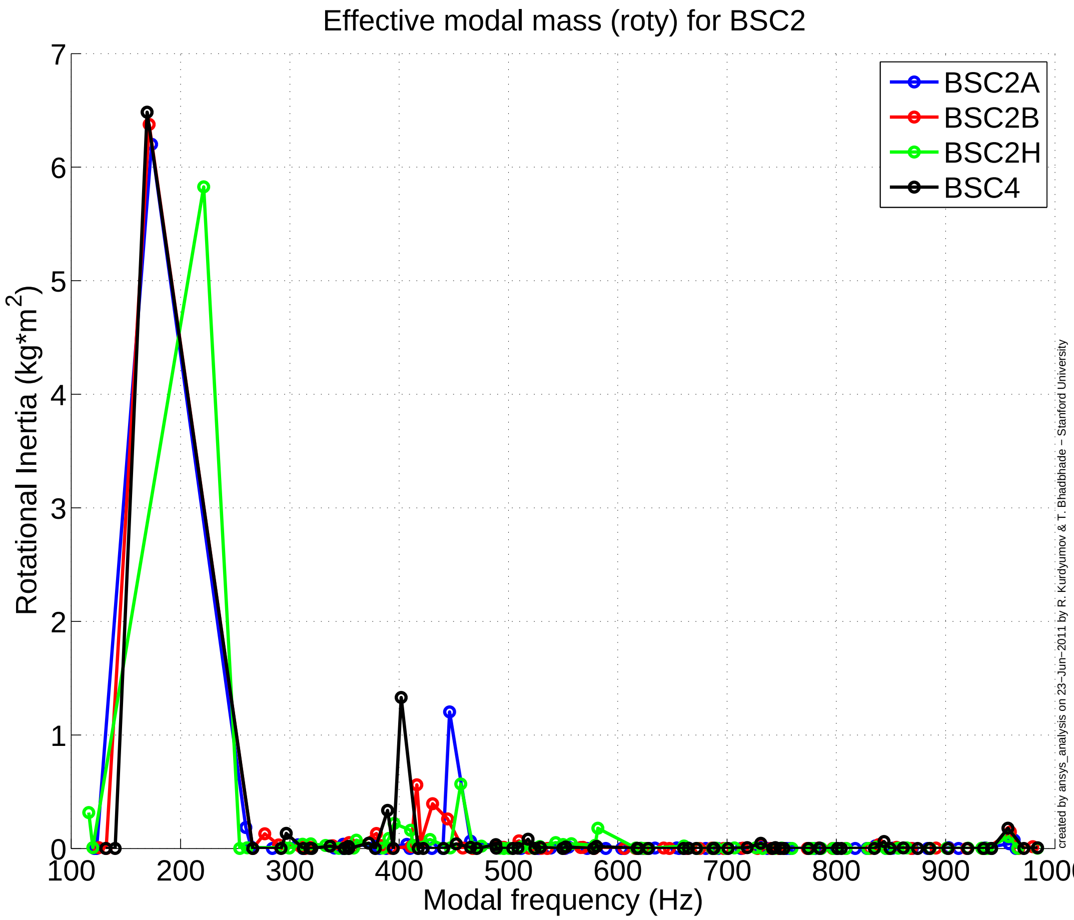

Effective modal mass (roty) for BSC2
Rotational Inertia (kg*m^2)
Modal frequency (Hz)
BSC2A
BSC2B
BSC2H
BSC4
created by ansys_analysis on 23−Jun−2011 by R. Kurdyumov & T. Bhadbhade − Stanford University

Figure 36

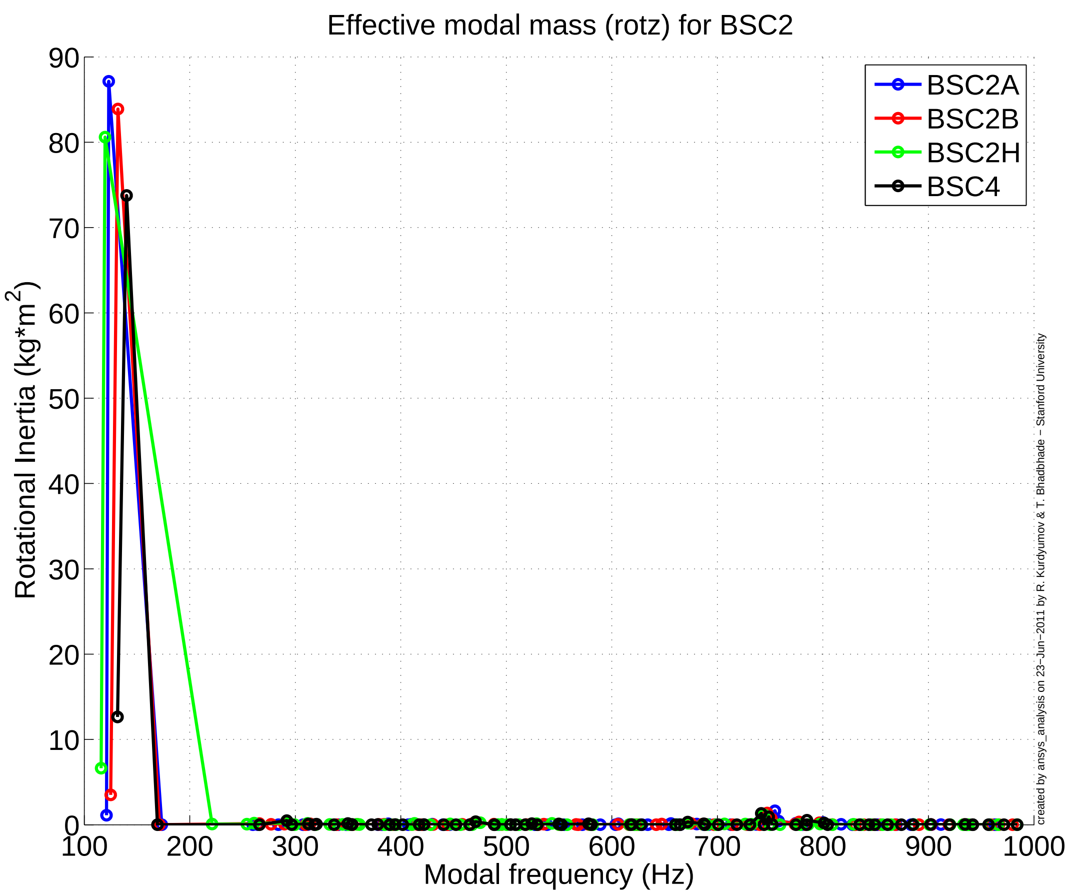

Effective modal mass (rotz) for BSC2
Rotational Inertia (kg*m^2)
Modal frequency (Hz)
BSC2A
BSC2B
BSC2H
BSC4
0
10
20
30
40
50
60
70
80
90
100
200
300
400
500
600
700
800
900
1000
created by ansys_analysis on 23−Jun−2011 by R. Kurdyumov & T. Bhadbhade − Stanford University

Figure 37

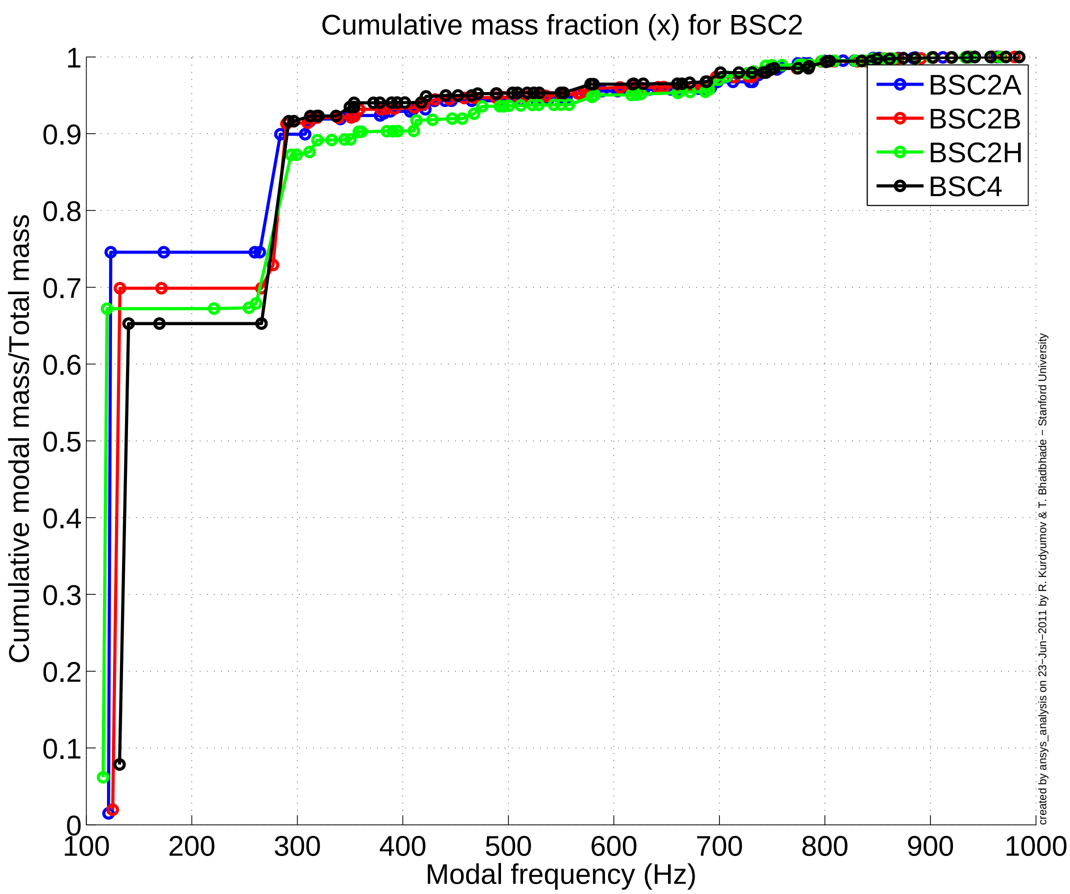

Cumulative mass fraction (x) for BSC2
Cumulative modal mass/Total mass
Modal frequency (Hz)
BSC2A
BSC2B
BSC2H
BSC4
0
0.1
0.2
0.3
0.4
0.5
0.6
0.7
0.8
0.9
1
100
200
300
400
500
600
700
800
900
1000
created by ansys_analysis on 23−Jun−2011 by R. Kurdyumov & T. Bhadbhade − Stanford University

Figure 38

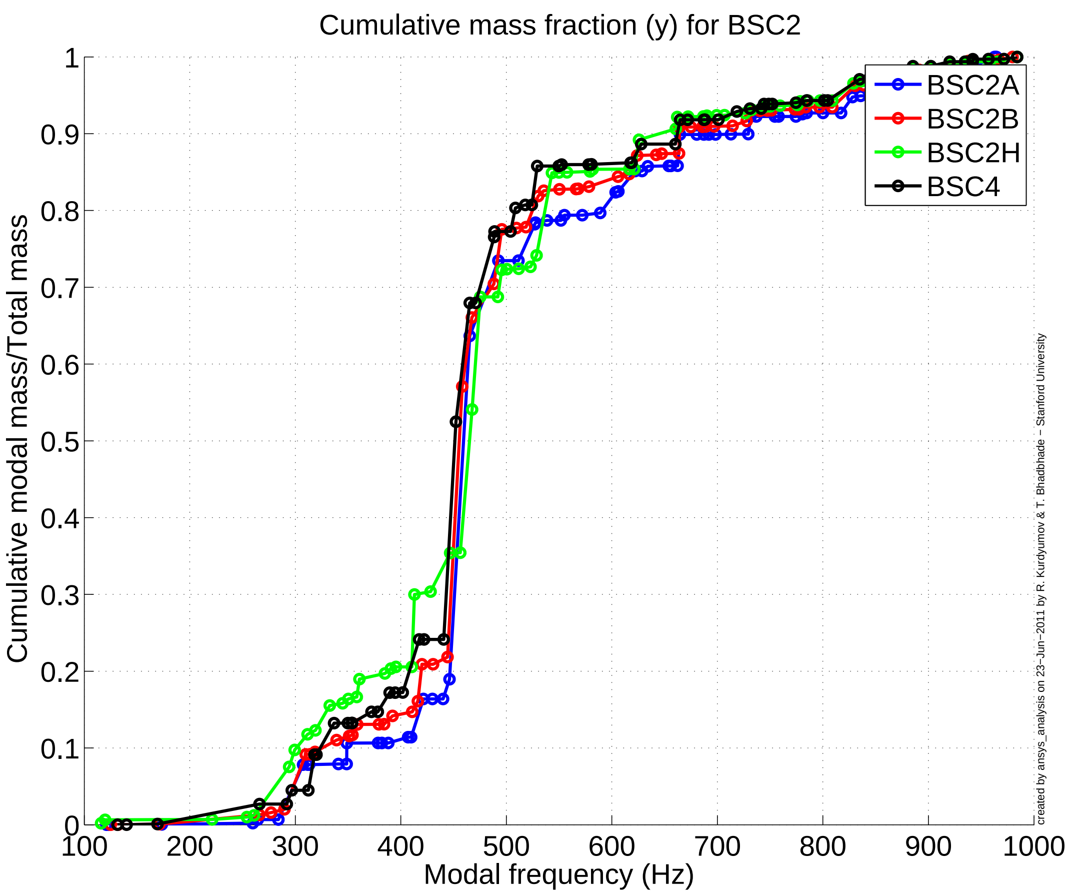

Cumulative mass fraction (y) for BSC2
Cumulative modal mass/Total mass
Modal frequency (Hz)
BSC2A
BSC2B
BSC2H
BSC4
0
0.1
0.2
0.3
0.4
0.5
0.6
0.7
0.8
0.9
1
100
200
300
400
500
600
700
800
900
1000
created by ansys_analysis on 23−Jun−2011 by R. Kurdyumov & T. Bhadbhade − Stanford University

Figure 39

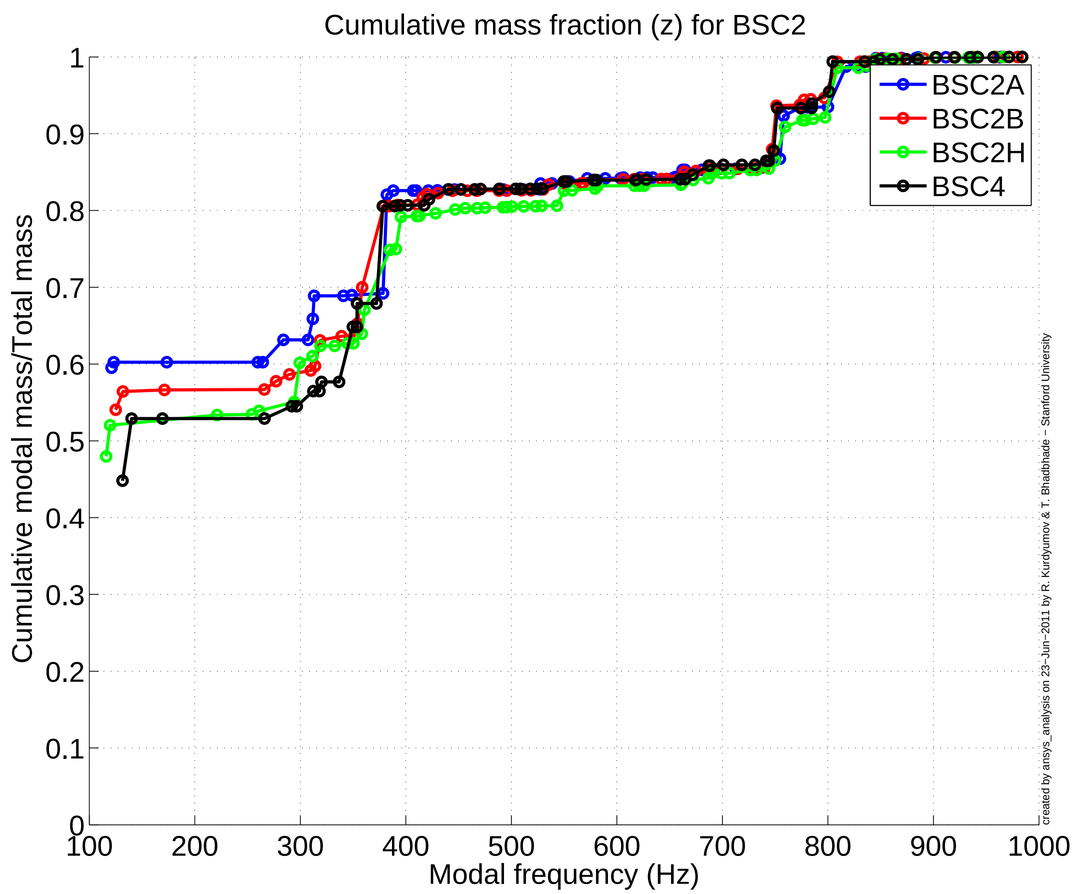

Cumulative mass fraction (z) for BSC2
Cumulative modal mass/Total mass
Modal frequency (Hz)
BSC2A
BSC2B
BSC2H
BSC4
0
0.1
0.2
0.3
0.4
0.5
0.6
0.7
0.8
0.9
1
100
200
300
400
500
600
700
800
900
1000
created by ansys_analysis on 23−Jun−2011 by R. Kurdyumov & T. Bhadbhade − Stanford University

Figure 40

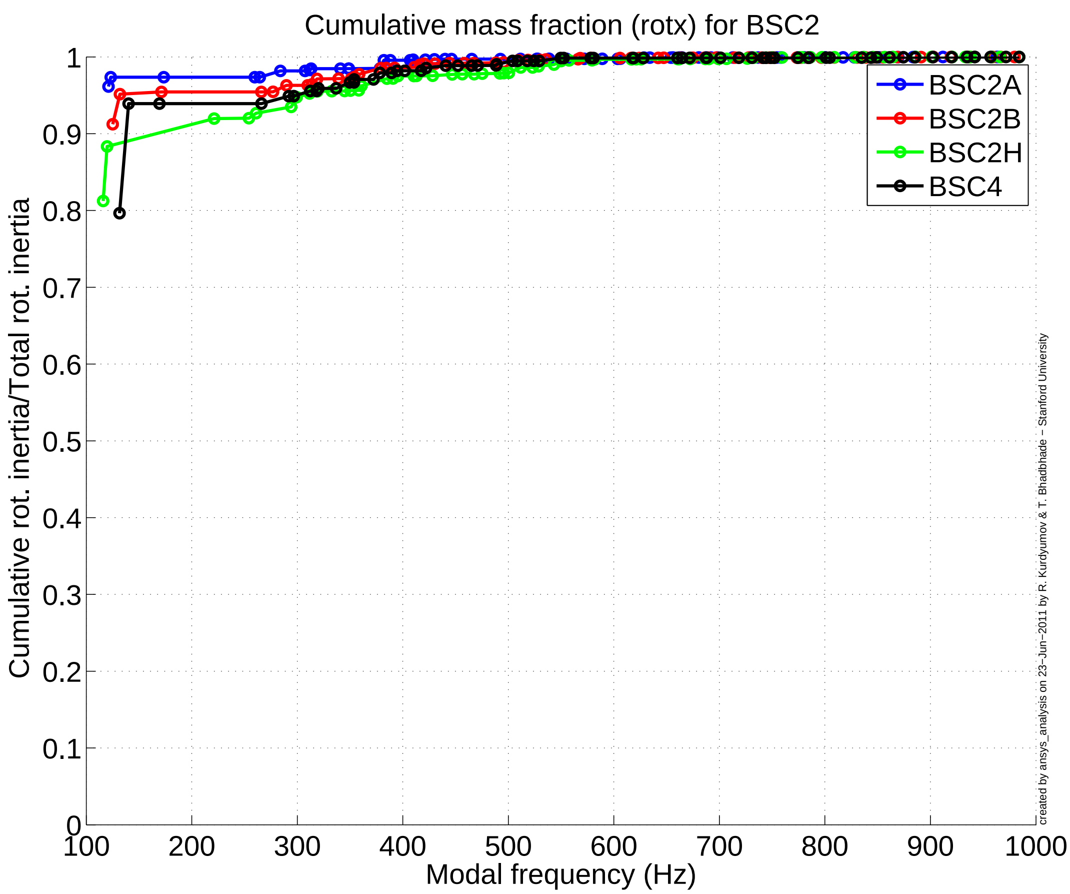

Cumulative mass fraction (rotx) for BSC2
Cumulative rot. inertia/Total rot. inertia
Modal frequency (Hz)
0
0.1
0.2
0.3
0.4
0.5
0.6
0.7
0.8
0.9
1
100
200
300
400
500
600
700
800
900
1000
BSC2A
BSC2B
BSC2H
BSC4
created by ansys_analysis on 23−Jun−2011 by R. Kurdyumov & T. Bhadbhade − Stanford University

Figure 41

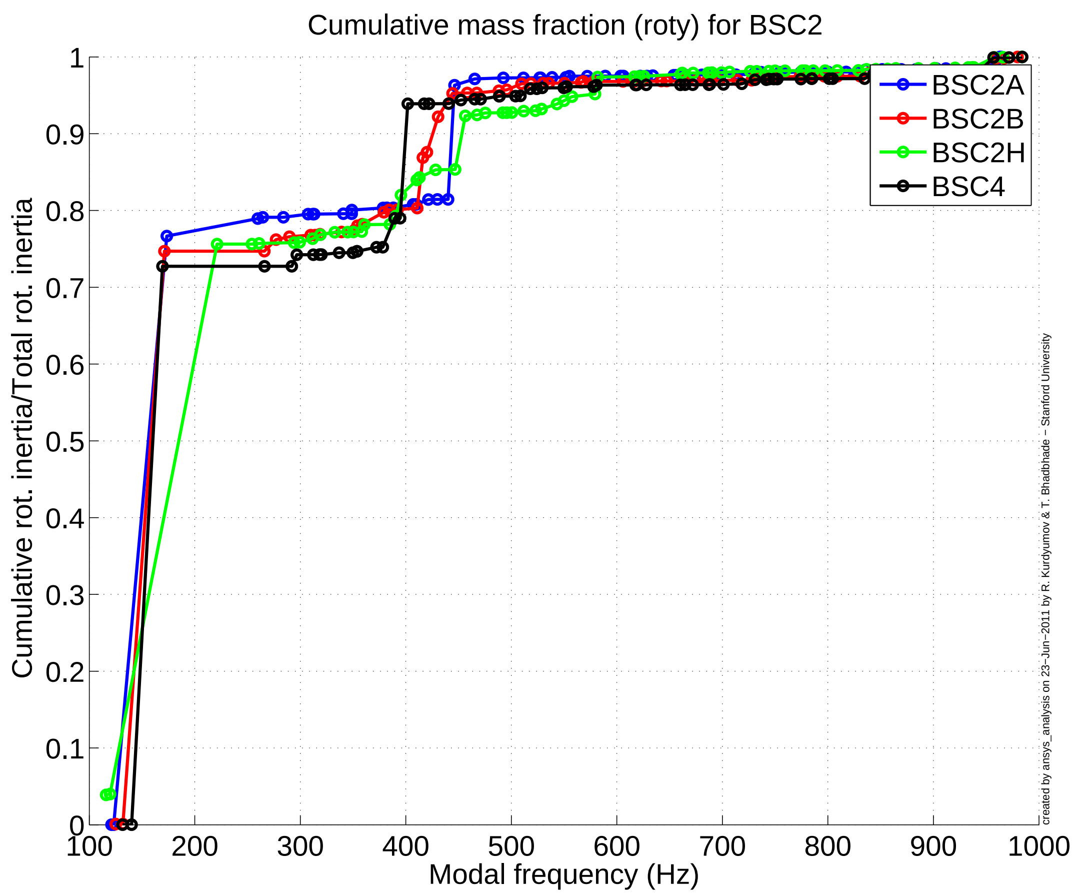

Cumulative mass fraction (roty) for BSC2
Cumulative rot. inertia/Total rot. inertia
Modal frequency (Hz)
BSC2A
BSC2B
BSC2H
BSC4
0
0.1
0.2
0.3
0.4
0.5
0.6
0.7
0.8
0.9
1
100
200
300
400
500
600
700
800
900
1000
created by ansys_analysis on 23−Jun−2011 by R. Kurdyumov & T. Bhadbhade − Stanford University

Figure 42

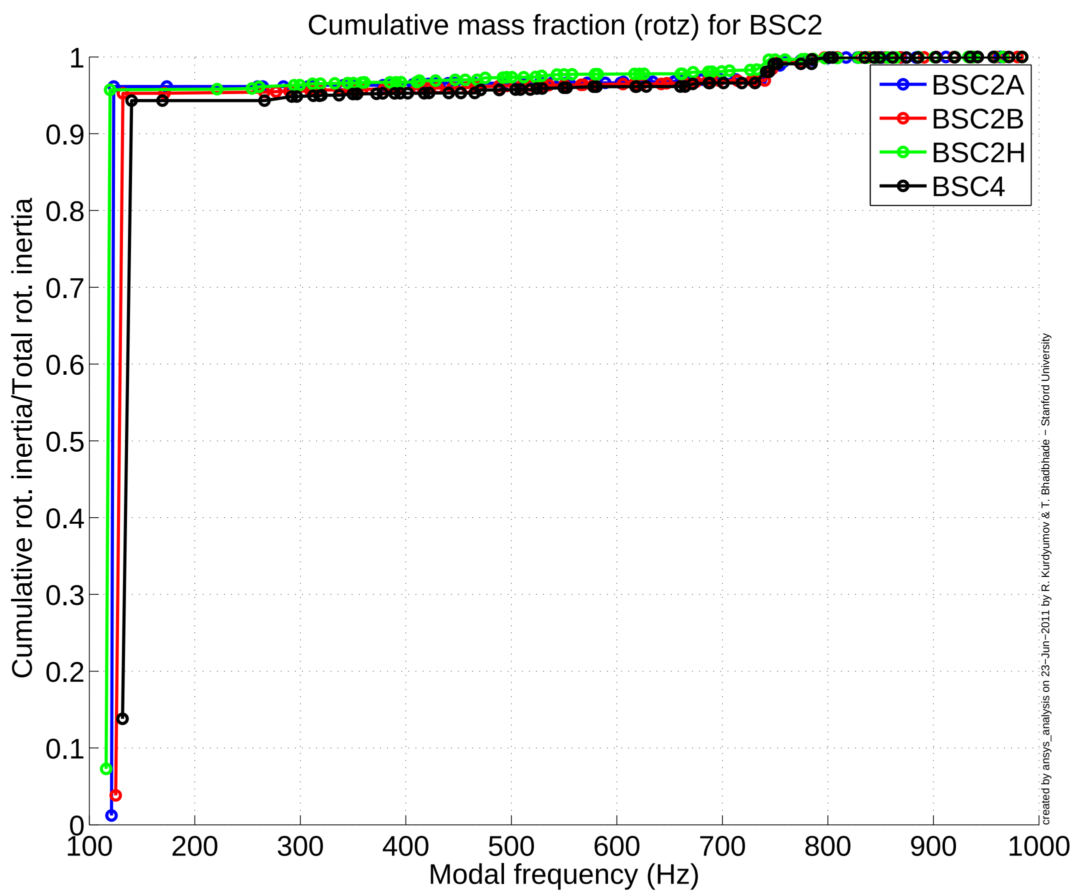
Cumulative mass fraction (rotz) for BSC2
Cumulative rot. inertia/Total rot. inertia
Modal frequency (Hz)
BSC2A
BSC2B
BSC2H
BSC4
0
0.1
0.2
0.3
0.4
0.5
0.6
0.7
0.8
0.9
1
100
200
300
400
500
600
700
800
900
1000
created by ansys_analysis on 23−Jun−2011 by R. Kurdyumov & T. Bhadbhade − Stanford University

Figure 43

A.5 Varying Fixed Supports Full Results

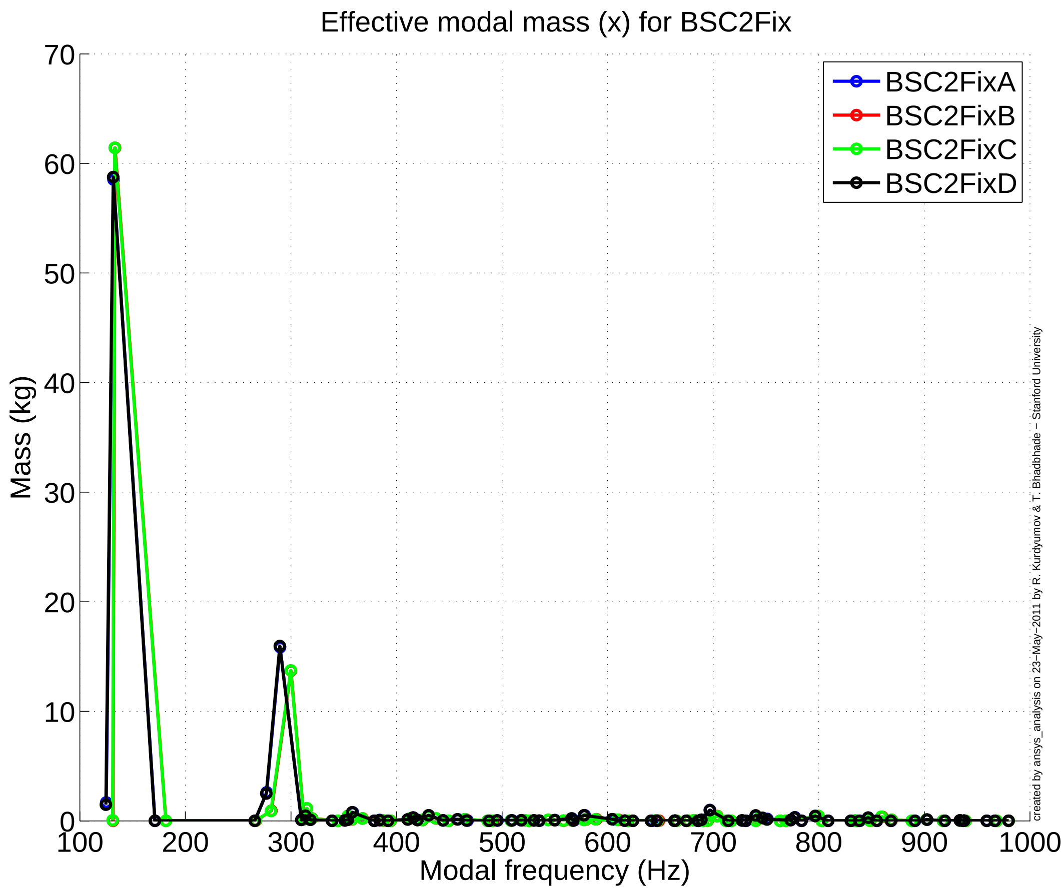

Figure 44

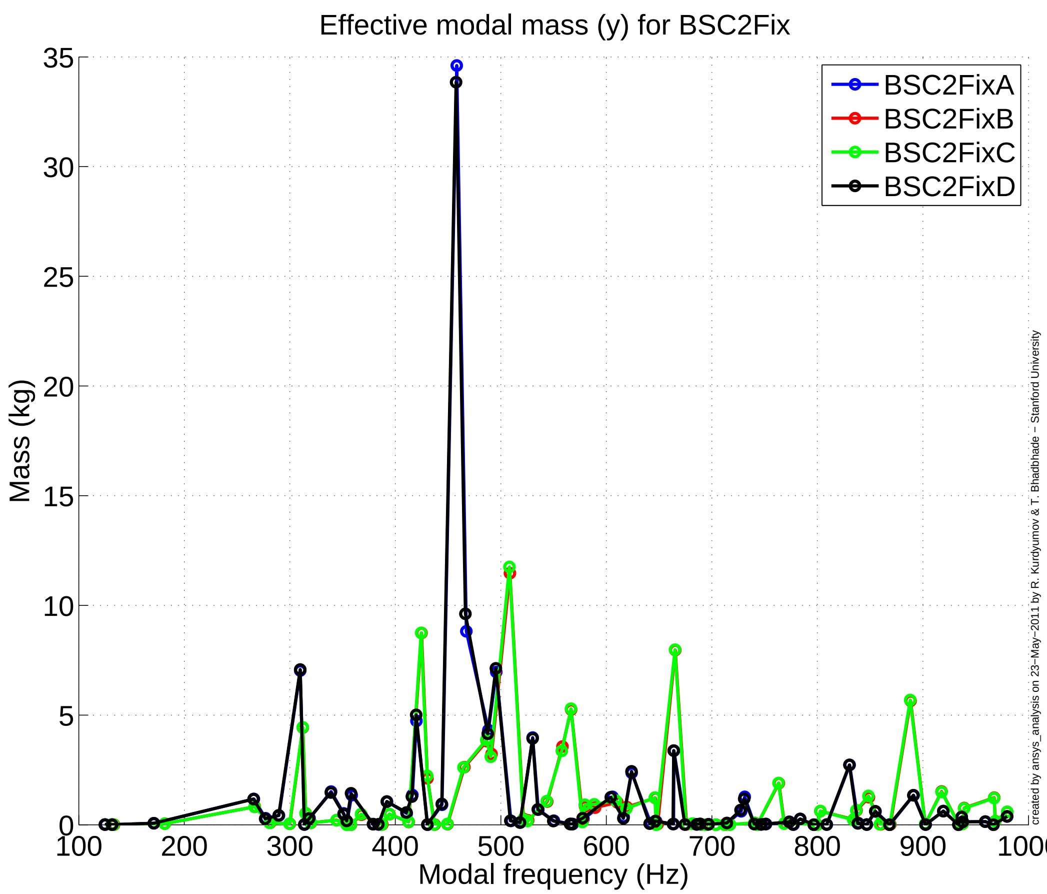
Effective modal mass (y) for BSC2Fix
Mass (kg)
Modal frequency (Hz)
BSC2FixA
BSC2FixB
BSC2FixC
BSC2FixD
0
5
10
15
20
25
30
35
100
200
300
400
500
600
700
800
900
1000
created by ansys_analysis on 23−May−2011 by R. Kurdyumov & T. Bhadbhade − Stanford University

Figure 45

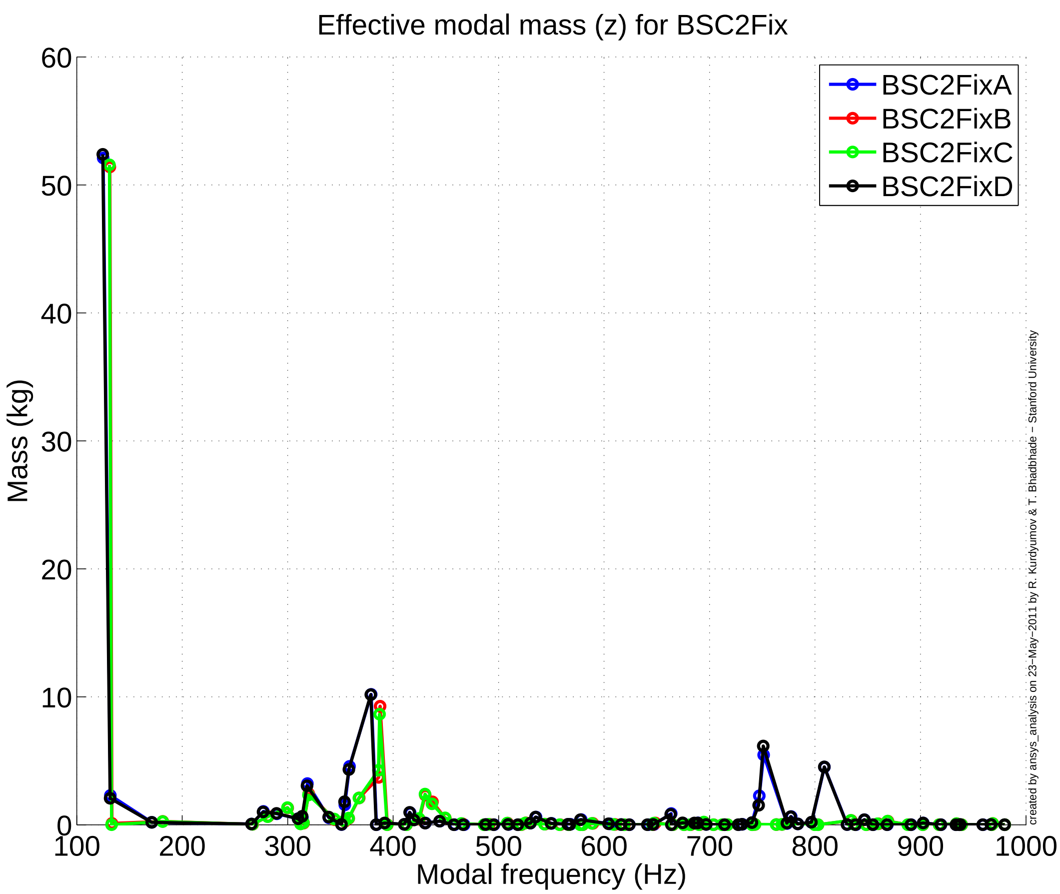
Effective modal mass (z) for BSC2Fix
Mass (kg)
Modal frequency (Hz)
0
10
20
30
40
50
60
100
200
300
400
500
600
700
800
900
1000
BSC2FixA
BSC2FixB
BSC2FixC
BSC2FixD
created by ansys_analysis on 23−May−2011 by R. Kurdyumov & T. Bhadbhade − Stanford University

Figure 46

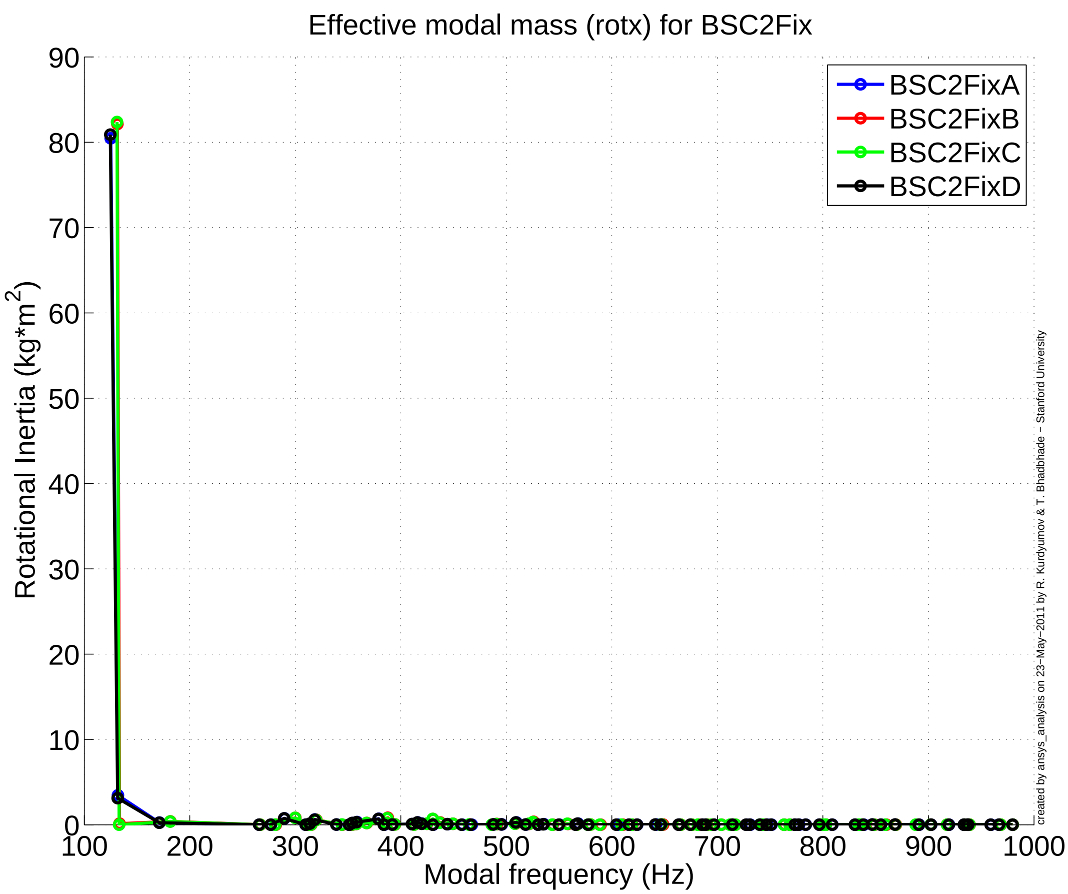

Effective modal mass (rotx) for BSC2Fix
Rotational Inertia (kg*m^2)
Modal frequency (Hz)
BSC2FixA
BSC2FixB
BSC2FixC
BSC2FixD
0
10
20
30
40
50
60
70
80
90
100
200
300
400
500
600
700
800
900
1000
created by ansys_analysis on 23−May−2011 by R. Kurdyumov & T. Bhadbhade − Stanford University

Figure 47

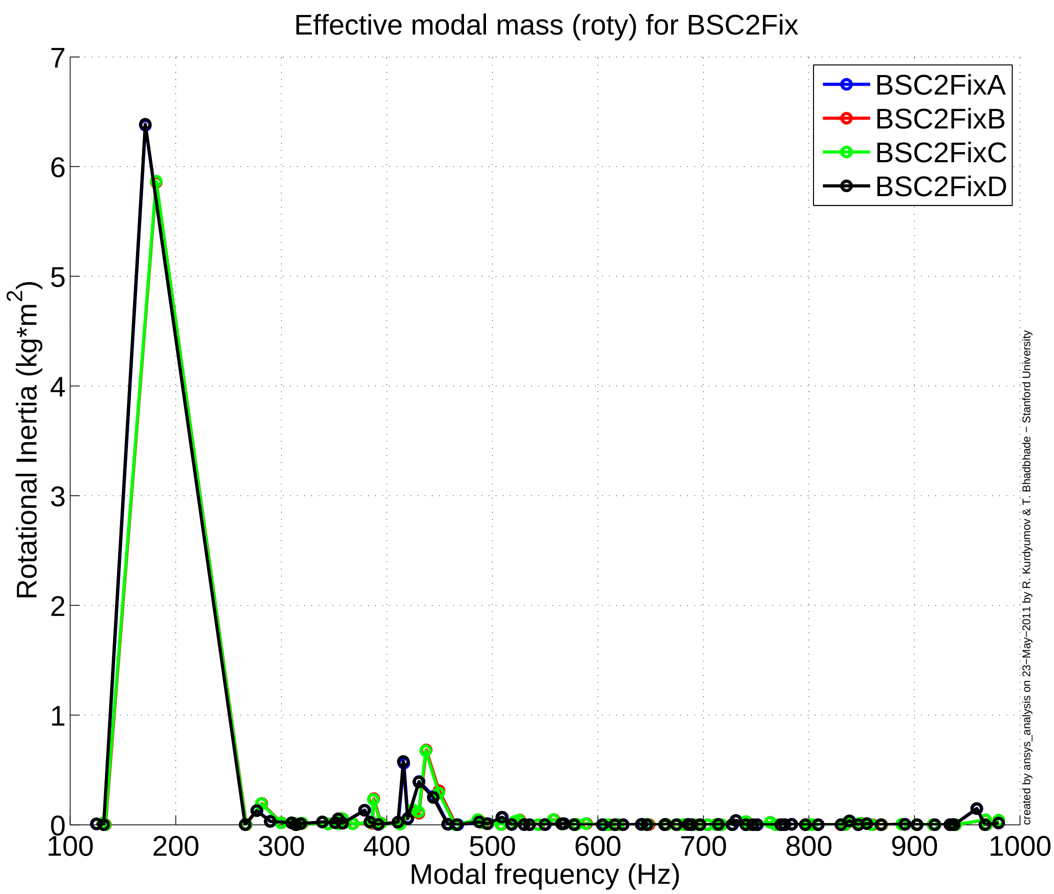
Effective modal mass (roty) for BSC2Fix
Rotational Inertia (kg*m^2)
Modal frequency (Hz)
BSC2FixA
BSC2FixB
BSC2FixC
BSC2FixD
0
1
2
3
4
5
6
7
100
200
300
400
500
600
700
800
900
1000
created by ansys_analysis on 23−May−2011 by R. Kurdyumov & T. Bhadbhade − Stanford University

Figure 48

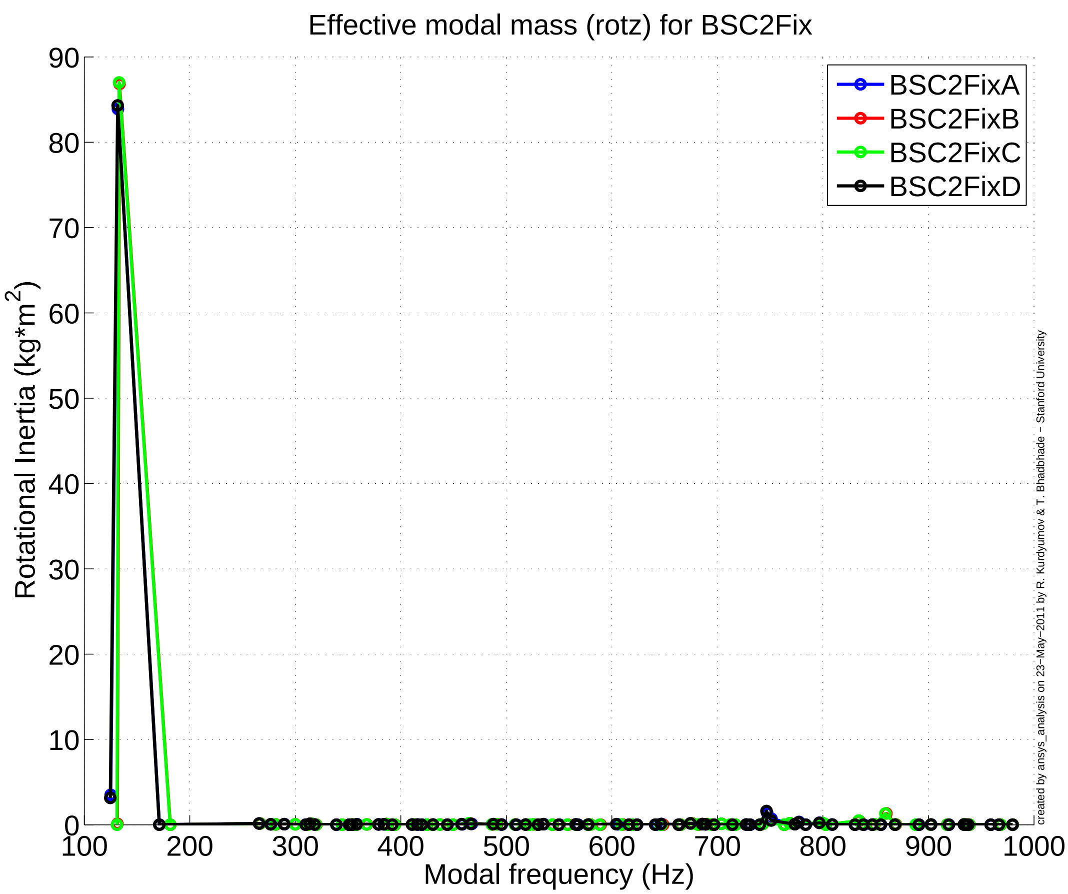

Effective modal mass (rotz) for BSC2Fix
Rotational Inertia (kg*m^2)
Modal frequency (Hz)
BSC2FixA
BSC2FixB
BSC2FixC
BSC2FixD
0
10
20
30
40
50
60
70
80
90
100
200
300
400
500
600
700
800
900
1000
created by ansys_analysis on 23−May−2011 by R. Kurdyumov & T. Bhadbhade − Stanford University

Figure 49

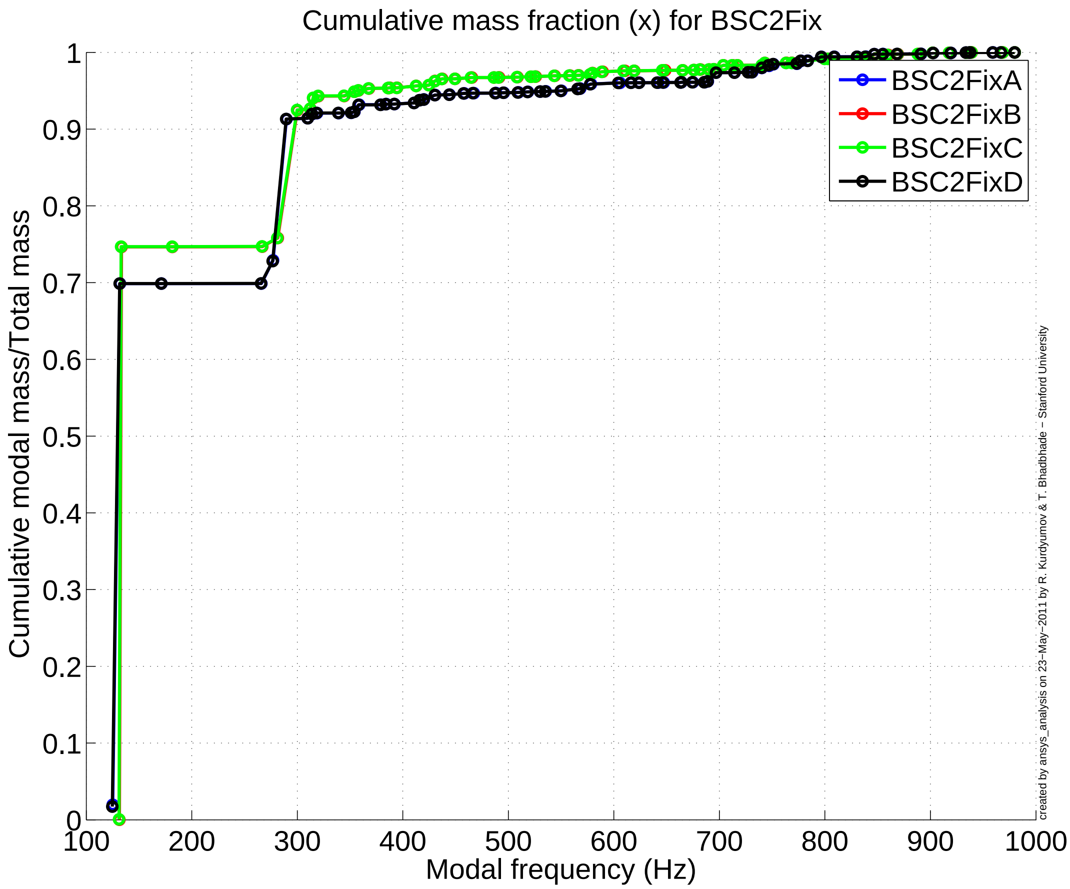

Cumulative mass fraction (x) for BSC2Fix
Cumulative modal mass/Total mass
Modal frequency (Hz)
BSC2FixA
BSC2FixB
BSC2FixC
BSC2FixD
0
0.1
0.2
0.3
0.4
0.5
0.6
0.7
0.8
0.9
1
100
200
300
400
500
600
700
800
900
1000
created by ansys_analysis on 23−May−2011 by R. Kurdyumov & T. Bhadbhade − Stanford University

Figure 50

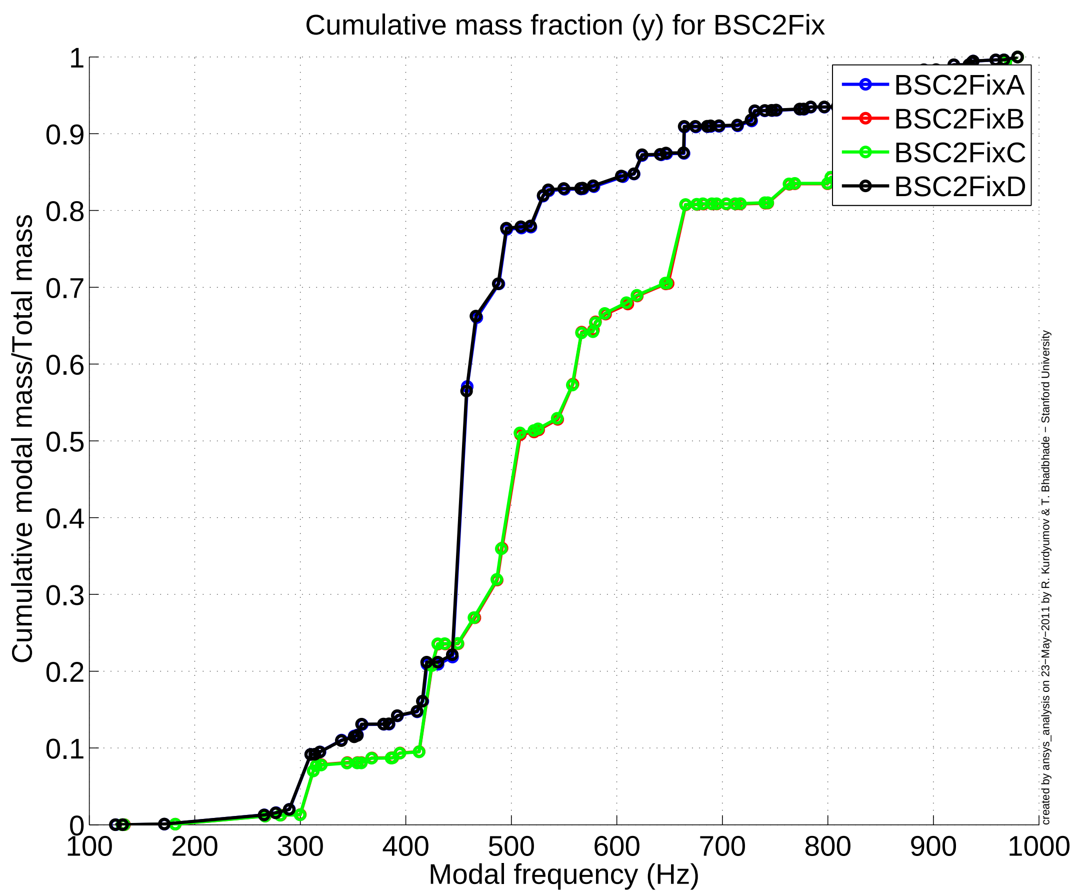

Cumulative mass fraction (y) for BSC2Fix
Cumulative modal mass/Total mass
Modal frequency (Hz)
BSC2FixA
BSC2FixB
BSC2FixC
BSC2FixD
0
0.1
0.2
0.3
0.4
0.5
0.6
0.7
0.8
0.9
1
100
200
300
400
500
600
700
800
900
1000
created by ansys_analysis on 23−May−2011 by R. Kurdyumov & T. Bhadbhade − Stanford University

Figure 51

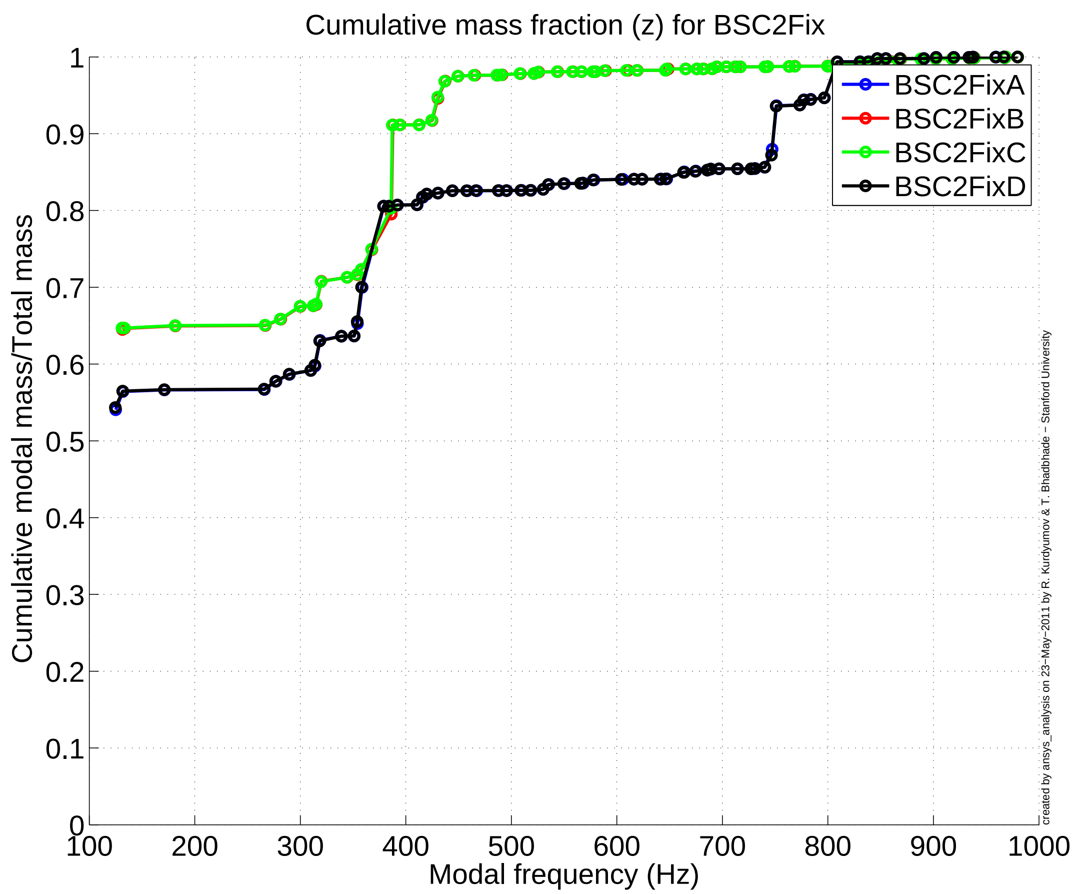
Cumulative mass fraction (z) for BSC2Fix
Cumulative modal mass/Total mass
Modal frequency (Hz)
BSC2FixA
BSC2FixB
BSC2FixC
BSC2FixD
0
0.1
0.2
0.3
0.4
0.5
0.6
0.7
0.8
0.9
1
100
200
300
400
500
600
700
800
900
1000
created by ansys_analysis on 23−May−2011 by R. Kurdyumov & T. Bhadbhade − Stanford University

Figure 52

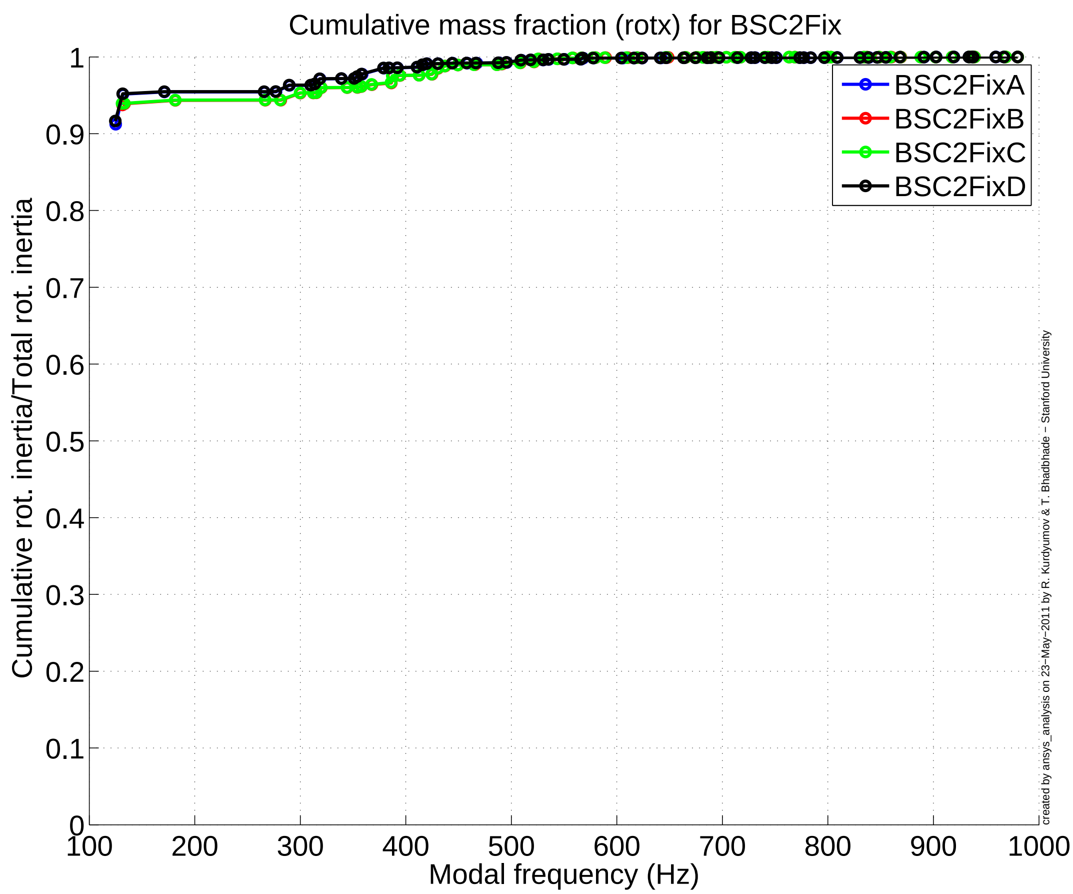
Cumulative mass fraction (rotx) for BSC2Fix
Cumulative rot. inertia/Total rot. inertia
Modal frequency (Hz)
BSC2FixA
BSC2FixB
BSC2FixC
BSC2FixD
0
0.1
0.2
0.3
0.4
0.5
0.6
0.7
0.8
0.9
1
100
200
300
400
500
600
700
800
900
1000
created by ansys_analysis on 23−May−2011 by R. Kurdyumov & T. Bhadbhade − Stanford University

Figure 53

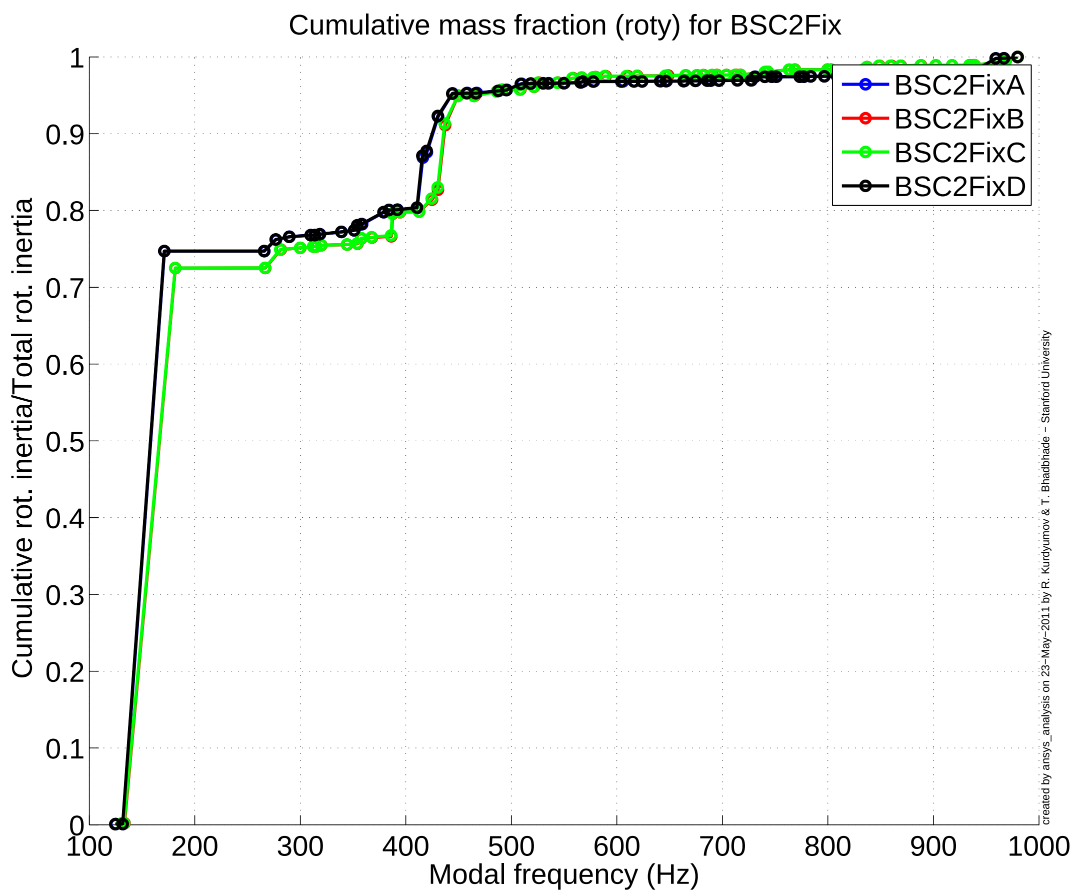

Cumulative mass fraction (roty) for BSC2Fix
Cumulative rot. inertia/Total rot. inertia
Modal frequency (Hz)
BSC2FixA
BSC2FixB
BSC2FixC
BSC2FixD
0
0.1
0.2
0.3
0.4
0.5
0.6
0.7
0.8
0.9
1
100
200
300
400
500
600
700
800
900
1000
created by ansys_analysis on 23−May−2011 by R. Kurdyumov & T. Bhadbhade − Stanford University

Figure 54

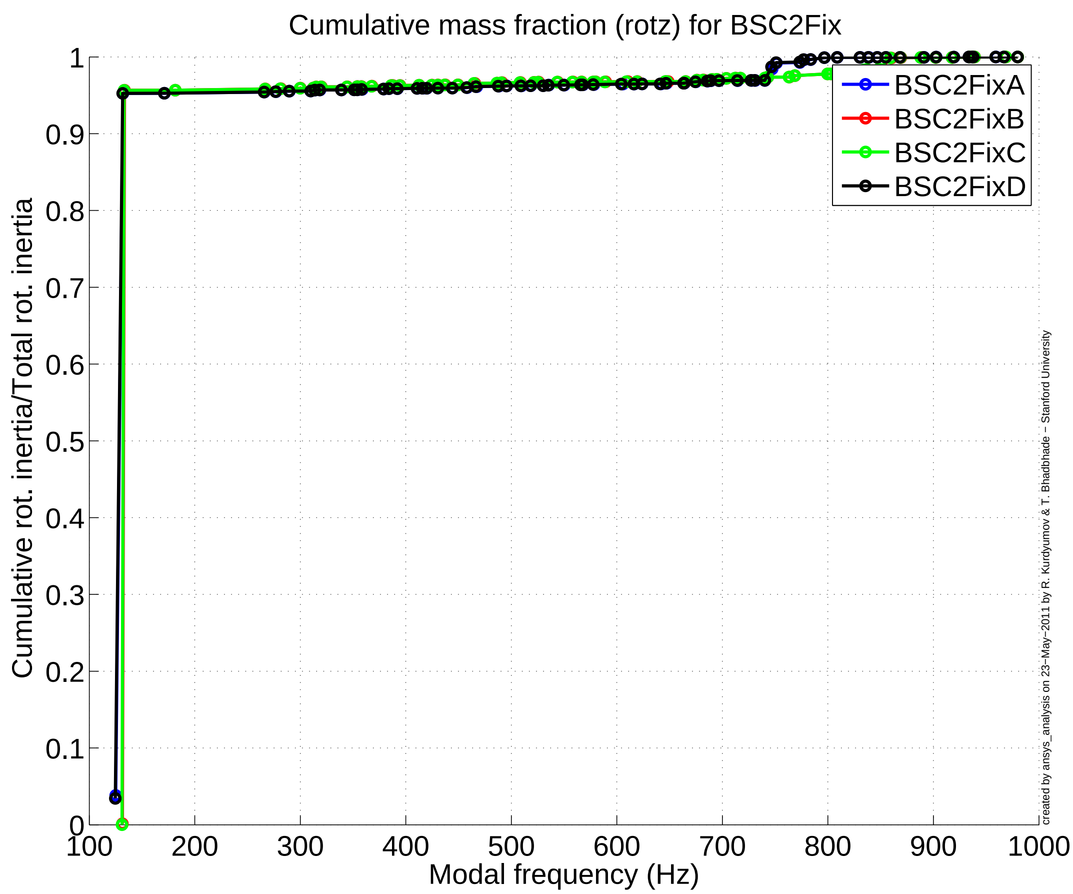
Cumulative mass fraction (rotz) for BSC2Fix
Cumulative rot. inertia/Total rot. inertia
Modal frequency (Hz)
BSC2FixA
BSC2FixB
BSC2FixC
BSC2FixD
0
0.1
0.2
0.3
0.4
0.5
0.6
0.7
0.8
0.9
1
100
200
300
400
500
600
700
800
900
1000
created by ansys_analysis on 23−May−2011 by R. Kurdyumov & T. Bhadbhade − Stanford University

Figure 55